Advance View
https://doi.org/10.3354/meps14330

MARINE ECOLOGY PROGRESS SERIES
Mar Ecol Prog Ser

July 6, 2023

Contribution to the Theme Section 'How do marine heatwaves impact seabirds?'

Marine bird mass mortality events as an indicator of the impacts of ocean warming

Timothy Jones[1,*], Julia K. Parrish[1], Jacqueline Lindsey[1], Charlie Wright[1], Hillary K. Burgess[1], Jane Dolliver[1], Lauren Divine[2], Robert Kaler[3], David Bradley[4], Graham Sorenson[4], Rémi Torrenta[4], Stacia Backensto[5], Heather Coletti[5], James T. Harvey[6], Hannahrose M. Nevins[6], Erica Donnelly-Greenan[6], David L. Sherer[7], Jan Roletto[8], Kirsten Lindquist[8,9]

[1]School of Aquatic and Fishery Sciences, University of Washington, Seattle, Washington 98105, USA
[2]Ecosystem Conservation Office, Aleut Community of St. Paul, Anchorage, Alaska 99503, USA
[3]Migratory Bird Management, US Fish and Wildlife Service, Anchorage, Alaska 99503, USA
[4]Birds Canada/Oiseaux Canada, Delta, British Columbia V4G 2T9, Canada
[5]Inventory and Monitoring Program, National Park Service, Fairbanks, Alaska 99709, USA
[6]BeachCOMBERS, Moss Landing Marine Laboratories, Moss Landing, California 95039, USA
[7]BeachCOMBERS, US Fish and Wildlife Service, Ventura, California 93003, USA
[8]Greater Farallones National Marine Sanctuary, NOAA, NOS, ONMS, San Francisco, California 94129, USA
[9]Greater Farallones Association, affiliate NOAA, NOS, ONMS, Greater Farallones National Marine Sanctuary, San Francisco, California 94129, USA

ABSTRACT: The frequency and severity of marine heatwaves (MHWs), an emergent property of global warming, has led to large-scale disruptions to marine ecosystems. As upper trophic species, marine birds reflect shifts in trophic structure and stability; therefore, a sharp increase in marine bird mortality is a clear signal of ecosystem impact. In this study, we analyzed 29 yr (1993–2021) of beached bird monitoring data (~90 000 surveys) to identify marine bird mortality events throughout the Northeast Pacific and Alaska, USA, and examined linkages to ocean–climate variability. Mortality events were documented throughout the study period, but massive events (>500 km in extent, >10 carcasses km^{-1}) occurred infrequently (n = 5), with an unprecedented sequence from 2014–2019. Event characteristics, including encounter rate (carcasses km^{-1}), duration, and spatial extent, were positively related to prior-year averaged sea surface temperature anomaly, with event magnitude (product of encounter rate, extent, and duration) displaying a step-like transition, increasing 5-fold between +0°C and +1°C above baseline (1981–2010) temperatures. Mortality events occurred more frequently following MHWs, and a common sequence of mortality events (at 1–6 and 10–16 mo after heatwave onset) was observed in the California Current large marine ecosystem following 3 prolonged MHW events. Following the second wave of mortality at 10–16 mo after MHW onset, a consistent 16 mo period of depressed carcass encounter rates ensued. Given continued global warming, our results point to more frequent large-scale mortality events and the potential for a new lower carrying capacity for marine birds in the Northeast Pacific.

KEY WORDS: Extreme events · Marine heatwaves · Citizen science · Seabird wrecks · North Pacific

1. INTRODUCTION

Marine heatwaves (MHWs) are a recently identified phenomenon (Hobday et al. 2016, Scannell et al. 2016, Carvalho et al. 2021) that are intensifying as the global climate warms as a direct response to human actions (Frölicher et al. 2018, Smale et al. 2019, Laufkötter et al. 2020). Prolonged MHWs have caused severe disruptions to associated marine ecosystems (Smith et al. 2023). In the Northeast Pacific,

*Corresponding author: timothy.t.jones@gmail.com

Publisher: Inter-Research · www.int-res.com

the 2014–2016 MHW that occurred as a result of anomalously low rates of heat loss from surface ocean waters is considered to be the largest and most prolonged MHW recorded to date (Holbrook et al. 2020). With peak extent covering an ocean area the size of Canada and intensity more than 4°C above climatology, the ecosystem impacts were profound, with documented effects on phytoplankton through to whales (Di Lorenzo & Mantua 2016, Suryan et al. 2021).

However, other periodic ocean warming phenomena are longstanding in this region. The El Niño–Southern Oscillation (ENSO) has been a stable feature on decadal to century scales (Braganza et al. 2009), with ecosystem impacts ranging up through marine birds and marine mammals (Hodder & Graybill 1985, Bertram et al. 2005, Häussermann et al. 2017). There is some evidence that these phenomena are linked, such that the impact of MHWs in this region may be extended by ENSO onset 6–12 mo later (Capotondi et al. 2022). To the north, within the Bering and Chukchi Seas, the transition to a multiyear warm stanza in 2014 (Stabeno et al. 2017), concurrent with the Northeast Pacific MHW of 2014–2016, was associated with dramatic shifts in sea ice extent, including the lowest sea ice minimum (2017–2018) and cold pool extent on record (1980–2019; Stabeno & Bell 2019). Arctic marine ecosystems generally (Stocker et al. 2013), and the Arctic region in particular (Grebmeier & Maslowski 2014, Huntington et al. 2020), appear to be in a period of rapid transition (Mueter et al. 2017, Stabeno & Bell 2019). Arctic sea surface temperatures (SSTs) are rising rapidly, and recent observations suggest that the Arctic climate is entering a 'new normal' (Jeffries et al. 2013, Wood et al. 2015).

Although MHWs are generally identified as discrete periods of prolonged (days-to-months) and significantly elevated ocean temperatures (Hobday et al. 2016), operational definitions now provide a standardized method for identifying and characterizing MHW events. Typically, MHWs are identified according to a minimum number of consecutive days during which temperatures exceed the 90th (or 99th; Holbrook et al. 2020) percentile of the 30 yr SST climatology (Hobday et al. 2016, Smale et al. 2019). In addition to capturing truly extensive, persistent events, such as the Northeast Pacific MHW of 2014–2016, the operational definition encompasses events across multiple ocean warming phenomena, including ENSO and Arctic warming, which collectively affect North Pacific marine ecosystems in profound ways.

Holbrook et al. (2020) suggested that 'skillful MHW prediction' could assist natural resource management, informing adaptation toward negative (e.g. exceeding thermal tolerances, Ledet et al. 2021; trophic mismatch, Piatt et al. 2020; increasing human–wildlife conflicts, Santora et al. 2020, Samhouri et al. 2021) and potentially positive (e.g. range extension; Sanford et al. 2019) impacts. However, at the spatiotemporal scale and intensity of the largest MHWs, what may be more important is understanding and predicting immediate and long-term ecosystem responses (e.g. Beaugrand et al. 2019) and whether and where tipping points of ecosystem change reside (Heinze et al. 2021). Understanding and forecasting those effects may be particularly important given that the incidence of MHWs has dramatically increased in the Northeast Pacific over the last 2 decades, with a 3-fold increase in intensity and a 9-fold increase in duration for those occurring in 2000–2022 compared to 1982–1999 (Barkhordarian et al. 2022).

In general, lower trophic levels should respond to bottom-up forcing more quickly than upper-level organisms. For instance, during the Northeast Pacific MHW of 2014–2016, abundance and size distribution of mesozooplankton in the Gulf of Alaska changed in 2014 soon after the MHW onset (Suryan et al. 2021, Batten et al. 2022). By contrast, upper trophic impacts were not apparent until 2015 (seabirds; Piatt et al. 2020) or beyond (Pacific cod *Gadus microcephalus*; Barbeaux et al. 2020). The delay in upper trophic response existed despite suggested differences in physiological response at the organismal level between homeotherms and poikilotherms, the latter of which may be expected to respond earlier, with potential to exacerbate effects on the former (Piatt et al. 2020). Thus, upper trophic response can be seen as an indicator of marine ecosystem impact following a MHW, as these long-lived and often wide-ranging species have life-history and natural-history flexibility ameliorating short-term environmental forcing (Burger & Piatt 1990, Johns et al. 2022).

Marine birds are excellent indicators of ecosystem change in response to both environmental and anthropogenic system forcing (Furness & Camphuysen 1997, Sydeman et al. 2021), as they are numerous, particularly in productive coastal waters (Nur et al. 2011), and are more easily observed and enumerated than their prey (Piatt et al. 2007a). As long-lived, strong trophic interactors (Cairns 1988, Österblom et al. 2006), marine birds integrate bottom-up forcing across space and time. Thus, marine bird vital rates are frequently used to infer changes in ocean productivity (Lee et al. 2007, Jessup et al. 2009, Avery-

Gomm et al. 2012). Sydeman et al. (2021) advocated for expanded monitoring of seabird breeding productivity, as this metric is correlated with ocean warming, particularly for piscivorous, surface-foraging species in the Northern Hemisphere. However, while breeding depression is most often provoked by bottom-up shifts in ocean productivity (Frederiksen et al. 2006, Suryan et al. 2006), other factors can also depress reproductive success. Among those, top-down forcing (e.g. Parrish et al. 2001, Gladics et al. 2015, Piatt et al. 2020) and direct environmental perturbations (i.e. storms and/or heat stress; Boersma & Rebstock 2014, Cook et al. 2020) can reduce breeding productivity, such that breeding depression is not always an indication of altered trophic dynamics. In addition, many species are buffered against ecosystem change via behavioral modification (Piatt et al. 2007b), dietary breadth (Sinclair et al. 2008), and/or prey switching (Watanuki et al. 2022). In comparison, a mortality signal in marine bird species, and specifically those that are an order, or orders, of magnitude above normal, is a clear indication of significant and substantial ecosystem impact.

In this paper, we gathered and analyzed 29 yr (1993–2021) of beached bird monitoring data (~90 000 surveys) to identify and characterize mortality events of marine birds throughout the Northeast Pacific and Alaska. Collated from 4 large-scale programs, the compiled data represent the most extensive record, in time and across space, of beached bird stranding events ever analyzed. We explored the association between marine bird mortality events and measures of ocean warming, as well as more specific characteristics associated with MHWs. In addition to definitively demonstrating that warmer than normal water is associated with marine bird mortality events, our goals were to understand whether there are thresholds to upper trophic response, including onset timing, duration, spatial extent, and overall mortality event magnitude, and whether there are fundamental response patterns across multiple mortality events.

2. MATERIALS AND METHODS

2.1. Beached bird data and processing

We sourced data from 4 beached bird monitoring programs: BeachCOMBERS (BCOMBERS: Central California, established 1997), Beach Watch (BWATCH: Central California, established 1993), the Coastal Observation and Seabird Survey Team (COASST: Northern California to Washington, and Alaska, USA, established in 1999), and the British Columbia Beached Bird Survey (BCBBS: Canada, established in 2002; Fig. 1). All 4 programs employ an effort-standardized survey protocol, whereby participants survey a fixed beach segment of known length for bird carcasses. Although participants are free to survey more frequently, they are asked to perform surveys at least monthly (BCOMBERS, COASST, BCBBS), or every 2 wk (BWATCH). As a result, the majority (82%) of surveys completed within 100 d of the previous survey on that beach segment (95% of all surveys) were done so within 10–40 d (Fig. S1 in Supplement 1 at www.int-res.com/articles/suppl/m14330_supp.pdf for all supplements). All participants are trained by relevant program staff.

A survey consists of a single-pass search of the beach, from the water's edge to the leading edge of vegetation. For each carcass encountered, species identity is determined via morphological (foot type), morphometric (tarsus, culmen, and wing chord measurements), and plumage characteristics, with the aid of a dichotomous beached bird key (Ainley et al. 1994, Hass & Parrish 2002). Following carcass identification, carcasses are photographed and either uniquely tagged (COASST) or marked (BCBBS, BCOMBERS, BWATCH) to identify them as a previously found carcass on subsequent surveys. Following each survey, data sheets and photographs are sent to program staff for verification and archiving.

Of the data available to us, we limited our analyses to surveys completed through 2021. We also excluded surveys from 3 regions: (1) south of 35.3° N in south-central California (BCOMBERS) due to the lack of long-term data (surveys began in 2013); (2) all beaches in Southeast Alaska (COASST) due to the exceptionally low carcass encounter rate in that region (42 birds across 1617 surveys, or 0.017 birds km^{-1}); and (3) the outer coast of British Columbia north of Tofino (49.16° N), as these locations were surveyed infrequently (Fig. 1). The remaining data encompassed 93 761 surveys across 1087 beach segments (Table S1 in Supplement 1). Data were screened to remove carcasses found and marked in a previous survey to avoid double counting. We retained carcasses independent of age group (adult, juvenile, fledgling, unknown age), as age was not recorded for the majority of species. Finally, we limited our analyses to species that are either entirely or seasonally dependent on the marine environment (hereafter marine birds), excluding all species that solely depend on terrestrial or freshwater environments and carcasses that could not be identified to any taxonomic level. These data were processed to create our base data set, which consisted

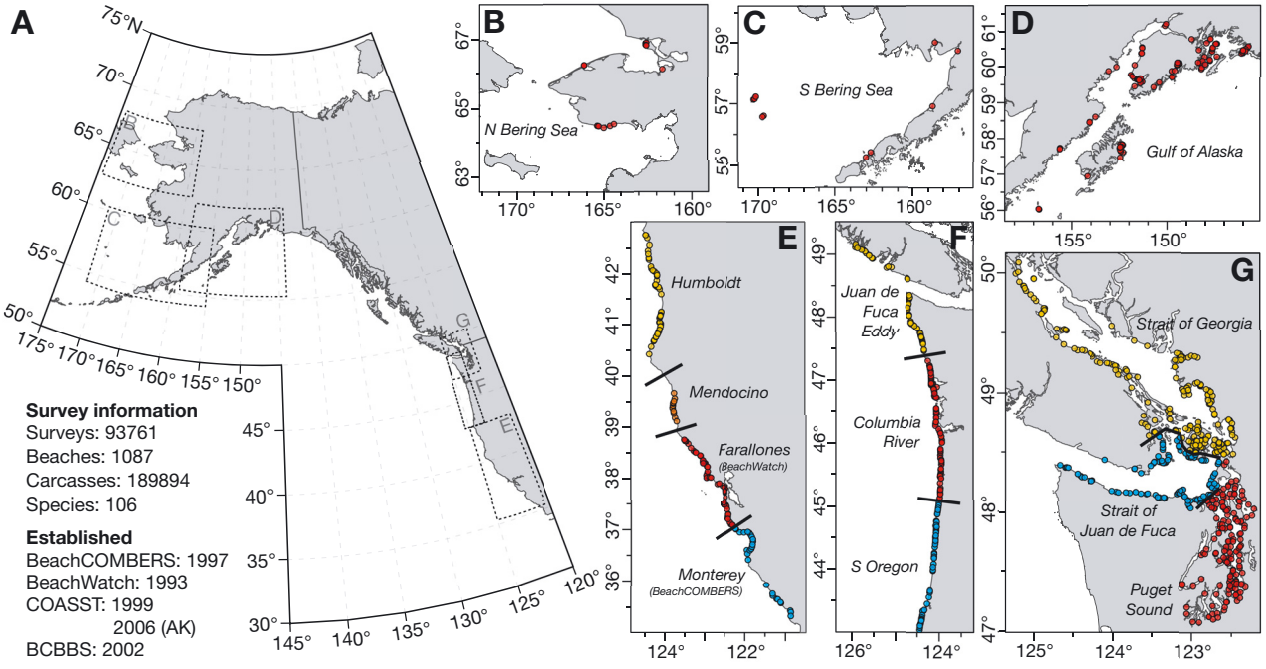

Fig. 1. (A) Beached bird program coverage in the North Pacific, along with insets for individual regions: (B) Northern Bering Sea; (C) Southern Bering Sea; (D) Gulf of Alaska; (E) central-northern California; (F) Oregon, Washington (USA), and the outer coast of Vancouver Island (Canada); and (G) Salish Sea. Colored points in (B–G) indicate locations of beach segments surveyed via effort-standardized beached bird surveys and are color-coded (E–G) to indicate regional delineations within the northern California Current large marine ecosystem. The majority of surveyed locations were part of the Coastal Observation and Seabird Survey Team (COASST) program, except beaches in Canada (BCBBS: British Columbia Beached Bird Survey) and central California (Beach Watch and BeachCOMBERS, indicated in E). Summary statistics presented in (A) are cumulative across programs

of survey-level counts of all newly found marine birds, beach length surveyed (km), survey interval (time since last survey in days), location (beach ID, latitude, longitude), and date.

In addition to regular beached bird monitoring data, we compiled information from opportunistic reports between 2017 and 2021 in the Bering and Chukchi Seas to bolster information from regions where regular monthly monitoring is scarce or absent (see Supplement 3). The majority of these data were communicated to the US Fish and Wildlife Service by coastal community members and/or Alaska Sea Grant Marine Advisors located in remote regions of northwest Alaska. While there was a concerted effort to record opportunistic reports following the mortality events in Alaska in 2015–2016, the reports were submitted voluntarily by individuals encountering marine bird carcasses. Therefore, opportunistic reports represent presence-only reports and are likely biased in space toward population centers that were aware of avenues for submitting reports. Reports were highly variable in the type(s) of information communicated; however, they always consisted of carcass counts or estimates at a given time and location. Due to concerns over spatial biases and lack of carcass-absence data, we included these data in event documentation and description but not statistical analysis.

2.2. Baseline model fitting

To model patterns in effort-standardized carcass abundance, we assigned the available data to one of 4 large marine ecosystems (LMEs): California Current (CCLME), Gulf of Alaska, Southern Bering Sea, and Northern Bering Sea/Southern Chukchi Sea (hereafter Northern Bering), based on survey location (Fig. 1). For the CCLME and Gulf of Alaska, we explored whether smaller regional subdivisions (~200 km) were necessary to capture seasonality and departures from baseline in beached bird abundance while avoiding spatio-temporal biases due to changes in survey coverage and extent within each LME. Because Southern and Northern Bering Sea surveys were concentrated in few locations, regional delineation was not attempted. Regional subdivisions were created based on major oceanographic or geographic features, such as river plumes and headlands (Fig. 1), beached bird abundance patterns, and

when surveys were established (Table S2 in Supplement 1). By comparing models with and without regional subdivisions, we found support for a subdivision within the CCLME but not for the Gulf of Alaska (Table S3 in Supplement 1). Therefore, models in the CCLME were fitted at the regional scale (Fig. 1E–G), whereas models for the Gulf of Alaska and Southern and Northern Bering Sea were fitted at the LME scale. For ease of language, we refer to the spatial scale of all models as 'region'.

For each region, we fitted generalized additive mixed-effects models (GAMMs) to the beached bird data in order to estimate baseline seasonality as a function of day-of-year as well as departures from baseline through time. Our models contained 2 major components. The first was a seasonal effect, modeled as a cyclic cubic spline of survey day-of-year. This accounted for seasonality that was consistently observed across years, with fitted values that were continuous (i.e. cyclic) across the year end–start boundary. Next, we divided time (1993–2021) into discrete 28 d periods and labeled surveys according to the period (starting from the earliest surveyed month; 1 Sep 1993) in which they occurred. A 28 d period was used as it matches the most frequently observed survey interval in our data set (Fig. S1 in Supplement 1). Departures from baseline were modeled by including 28 d period as a random effect, allowing the fitted values for each period to fluctuate about long-term seasonality. The magnitude and direction of these random effects indicate to what extent carcass encounter rates (carcasses km^{-1}) were above or below baseline for each period. Given that, we refer to this term as 'encounter rate anomaly'.

We used a negative binomial (NB) GAMM (log-link function) with an offset term to account for differing beach lengths and a random effect of beach to account for consistent variability among beaches:

$$\ln(\mu_{i,j}) = \beta_0 + s(d_i) + \delta_{t_i} + \gamma_j + \ln(L_{i,j}) \quad (1)$$

$$C_{i,j} \sim \mathrm{NB}(\mu_{i,j},\theta) \quad (2)$$

where $C_{i,j}$ is the observed carcass count on survey i on beach segment j, $\mu_{i,j}$ is the expected count, β_0 is the intercept, $s(d_i)$ is the seasonal smooth term of day-of-year, d_i, δ_{t_i} is the random effect of time-period t_i (i.e. anomaly) within which the survey occurred, γ_j is the beach random effect, $L_{i,j}$ is beach length surveyed, and θ is the negative binomial dispersion parameter. Within this model, random effects are normally distributed on the log-scale (log-link), such that:

$$\gamma_j \sim N(0,\sigma_\gamma) \quad (3)$$

where σ_γ is the standard deviation of beach random effects. However, temporal random effects were assumed to be autocorrelated through time, which we model via an AR1 process:

$$\delta_t = \rho\delta_{t-1} + e_t \quad (4)$$

$$e_t \sim N(0,\sigma_t) \quad (5)$$

where ρ is the lag-1 autocorrelation strength and e_t are the residuals of this process, assumed to be normally distributed with standard deviation σ_t. Specifying autocorrelated random effects allowed for anomalies to persist through time and addresses the assumption of independence among random effects that would otherwise be violated.

Given the log-link function, random effects are log-normally distributed on the response (encounter rate) scale, allowing for positive deviations (i.e. elevated encounter rates) that are naturally more extreme than negative deviations (i.e. depressed encounter rates). For the same reason, random effects are multiplicative, such that anomaly estimates of ±1 represent encounter rates that are $e^{\pm 1}$ = 0.37 (–) and 2.71 (+) times baseline, providing a natural way to classify departures from baseline.

In addition to these core model components, we also considered the fixed effects of beached bird program and survey interval to control for differences in survey protocol and carcass accumulation time between surveys, respectively. For each region, we compared models with and without these additional terms (program effects were only suitable in regions with overlapping programs; Fig. 1) and chose the most parsimonious model (i.e. that with the lowest Akaike's information criterion adjusted for small sample sizes, AICc) for each region to perform all subsequent analyses with (Table S4 in Supplement 1).

Models were fitted using Stan (Stan Development Team 2022a) and RStan (Stan Development Team 2022b), the R interface to Stan. Model parameters were defined via vague priors and estimated using 4 Markov chain Monte Carlo chains, each running for 12 000 iterations split equally between warm-up and estimation phases. Model parameter convergence was evaluated based on traceplots and convergence criteria (R-hat ≤ 1.05; Vehtari et al. 2021). Models were further evaluated by checking that random effects distributions met the assumptions of normality, and model fit was checked through comparisons between observed and fitted values before proceeding with subsequent analyses (Supplement 2).

2.3. Event identification and classification

Mortality events were first identified at the region level based on model-estimated encounter rate anomalies. Regional events were identified as one or more contiguous time periods (i.e. 28 d) where the encounter rate was estimated to be at least twice baseline. Following that, we excluded all matching incidences where fewer than 50 carcasses were observed, removing cases that were a reflection of low and/or localized survey effort.

For each regional mortality event, a series of characteristics were calculated by either summing or averaging across time period (28 d) specific model estimates within the event time window (Table S6 in Supplement 4). These were (1) 'duration', calculated as time-period count multiplied by 28; (2) 'average encounter rate', calculated as mean across time-period-specific encounter rate estimates; (3) 'average anomaly', defined as mean across-encounter-rate anomalies, and converted into relative units:

$$\exp\left(\frac{1}{n_e}\sum_{i}^{n_e}\delta_i\right) \quad (9)$$

where n_e is the number of time periods within the event, and therefore represents the average relative departure from baseline; and (4) 'extent', defined as the event spatial coverage. Extent was calculated by first estimating the proportion of beaches within the event region where the observed count on any survey throughout the event duration was at least 3 times higher than the baseline expected count for that survey. This provided a measure of the coverage or ubiquity of elevated abundances, separating localized events from region-wide events. Due to differences in region extent, we then multiplied this proportion by the maximum point-to-point distance (km) between beach segments within each region as a measure of overall region size. We examined how this point-to-point distance varied through time due to the addition or removal of sites, and in most regions, it reached an asymptotic value as survey coverage became more comprehensive (Fig. S16 in Supplement 4). For each region, we chose the asymptotic value as a constant value to be applied in all extent calculations to avoid a perceived increase due to expanding survey coverage. Extents were not calculated for the Salish Sea regions due to the complex nature of the associated coastlines, or for the Northern or Southern Bering Sea due to the lack of comprehensive coverage (Fig. 1).

Following extent calculations, event 'magnitude' was calculated as the product of average carcass encounter rate, extent, and duration. This measure integrates carcass encounter rate over relevant space and time and can therefore be used to compare collective relative magnitudes among events. However, it should not be interpreted as cumulative deposition (i.e. the product of carcasses km^{-1} survey^{-1} × km × days), as it omits factors necessary to convert carcass counts to deposition (Jones et al. 2017).

Mortality events were also sorted into 4 encounter rate categories. This was based on average encounter rate and anomaly relative to baseline (Table 1). Category 1 events were just abo ve our minimum threshold of twice baseline. By contrast, Category 4 events represented only the most severe carcass encounter rates: anomalies greater than 5 times the baseline and averaging at least 8 carcasses km^{-1}.

Given the separation of US/Canadian coastlines outside of Alaska into distinct regions, single expansive events were documented multiple times in different regions if the event crossed regional boundaries. We therefore combined regional events into a smaller number of distinct events. This was based on location, requiring that they occur within the same LME; timing, requiring that event mid-points be separated by <90 d; and taxonomic composition, requiring that they be categorized in the same event typology based on a hierarchical cluster analysis of taxonomic composition among regional events (see Supplement 4). Aggregated event characteristics were then calculated by either averaging (encounter rate, duration) or summing (extent, magnitude) across constituent regional event values.

2.4. SST data and MHW identification

SST data were obtained from the NOAA OI SST V2 High Resolution Dataset (daily, spatial resolution: 0.25°; Reynolds et al. 2002) for 1981–2021, inclusive. For each region, we defined a bounding box from the corresponding shoreline out to 100 km offshore and calculated the average SST within that area for each

Table 1. Thresholds of average encounter rate and average anomaly (multiplication factor relative to seasonal base lines) used to categorize mortality events

Category	Average encounter rate (carcasses km^{-1})	Average anomaly (× baseline)
1	>1	>2
2	>2	>3
3	>4	>4
4	>8	>5

day between 1981 and 2021. The resulting time-series of regional SST values was then smoothed using a 30 d Gaussian kernel smooth after Hobday et al. (2016). From this, we calculated the region-averaged 30 yr climatology (1981–2010) by taking the mean regional SST for each calendar day-of-year. We then converted regional SST time-series to SST anomaly (SSTa) by subtracting the climatological average. For each mortality event identified from beached bird data, we calculated the mean SSTa value for the corresponding region(s) averaged over the year prior to mortality event onset (onset date – 360 to onset date, inclusive) providing a measure of temperature conditions prior to the event. The resolution of SST data prevented calculations within the Salish Sea. For the single mortality event identified in the Salish Sea, we instead used SST data from the Juan de Fuca Eddy region (Fig. 1), as that mortality event extended from the Strait of Juan de Fuca to the outer coast of northern Washington.

In addition, we used SST data at the regional and LME scale (<100 km offshore) to identify MHW days (SST > 90^{th} climatological percentile for that day-of-year) and MHW episodes (contiguous period of at least 6 MHW days, allowing for a maximum 2 d break) following the methods of Hobday et al. (2016). For each MHW episode, we calculated onset and termination dates as well as average intensity (mean SSTa).

In all instances, associated SST and MHW results should be interpreted within the context of large-scale (200–1000 km) temperature perturbations given the spatial scale of our analyses.

2.5. Aggregated event characteristics and connection to SSTa

Aggregated event statistics (average anomaly, average encounter rate, extent, duration, magnitude; averaged or summed across constituent regional events) were used to identify whether event characteristics had changed throughout the study period. To do this, we fit linear models with time as the single predictor variable, using weighted least squares with an exponential variance function ('varExp' in the 'gls' function in R; Pinheiro & Bates 2022) to control for heteroscedasticity that was evident upon examining the data. We then used bootstrap resampling (n = 1000 permutations) to estimate the 95% confidence intervals of model coefficients regarding event characteristic trends through time.

We also investigated whether there was a relationship between aggregated event characteristics and prior-year averaged SSTa. We used the same modeling process as described for trends through time but also included season (winter: Dec–Feb, spring: Mar–May, summer: Jun–Aug, autumn: Sep–Nov) as a factorial variable based on event onset date. For both time and SSTa analyses, we fitted models to characteristics data from all aggregated events as well as to a reduced data set that did not contain Category 1 events (Table 1) to identify whether patterns were more evident for higher encounter rate mortality events.

To determine whether there were thresholds in SSTa associated with mortality event severity, nonlinear relationships between aggregated event magnitude and SSTa were explored. We fitted shape-constrained (SC-GAM; Pya 2022) and ordinary generalized additive models (GAMs; Wood 2017), using the 'scam' and 'gam' functions in the 'scam' and 'mgcv' packages in R, respectively (Wood 2017). The former approach allows for specification of monotonic functions between SSTa and event magnitude that are likely to be more representative of real-world functional relationships. We compared AICc between 4 different models for event magnitude: a null model, an unconstrained GAM with SSTa as a smooth term, and 2 SC-GAMs, each containing SSTa effects via a smooth term but differing with regard to functional constraints (monotonic increase, monotonic decrease). The best-fitting model (lowest AICc) was used to estimate the difference in event magnitude between SSTa = 0°C and SSTa = 1°C. Furthermore, functional thresholds were also calculated from the fitted function by calculating the SSTa value where model-estimated magnitude approached within 10% of its minimum (lower threshold) and maximum (upper) values. These thresholds provide measures of SSTa below or above which we would expect lower or larger magnitude events, respectively. Confidence intervals for these thresholds were determined via posterior simulation (Simpson 2022).

2.6. MHW association analyses

If mortality events are associated with MHWs, they should occur more frequently following MHW onset than would be expected by chance. To test this hypothesis, regional mortality events were linked to the most recent MHW. We calculated 2 test statistics from these data: the number of mortality events occurring within 12 mo of a MHW and the mean time delay, both based on time between MHW onset and mortality event onset dates. We then created a procedure where mortality events were randomly re-

arranged in time to represent the occurrence of mortality events de-coupled from MHWs and then calculated the corresponding statistics for each realization of this randomization process (for details see Supplement 6). Null distributions of our test statistics were constructed based on 1000 repetitions of this procedure, and we used this to calculate p-values and the 95% range of values expected under the null hypothesis that mortality events occurred at random with respect to MHWs. We performed this test procedure using encounter rate Category 2–4 events as well as only using Category 3–4 events to determine whether results differed when considering only the most extreme events.

2.7. Comparison of impacts between prolonged MHWs

To explore the degree to which there is a system-level pattern of response to MHWs, we focused on the progression of beached bird encounter rates, before, during, and after 3 prolonged MHWs in the Northeast Pacific: the 1997–1998 ENSO event (Humphries et al. 2015), the 2014–2016 Northeast Pacific MHW (Di Lorenzo & Mantua 2016), and the 2018–2019 ENSO event (Chen et al. 2021).

We examined the time series of encounter rate anomalies from 6 mo before through 4 yr after the onset of each MHW to identify whether, and for how long, beached bird abundances and phenology were disrupted following MHW occurrence. We limited these exploratory analyses to the central California Current regions, as monitoring elsewhere was established after the 1997–1998 ENSO event.

All analyses were performed in R version 4.2.1 (R Core Team 2022).

3. RESULTS

3.1. Event identification and aggregation

Across the 13 regions examined, 28 d encounter rate anomalies (hereafter anomalies) exceeded the 2× baseline threshold for 11.7% of the 3119 region × time periods examined (Fig. 2). These were not equally spread among regions and ranged from 0–4% in the sheltered waters of the Salish Sea to 26% in the Southern Bering Sea (Fig. 2A). Grouping contiguous 28 d periods resulted in the identification of 111 region-specific events (Fig. 2A). The majority (82%) of regional mortality events identified were constituents of broader-extent events spanning multiple regions (Fig. 2A). Grouping regional mortality events based on timing, location, and taxonomic composition (Fig. S18 in Supplement 4) resulted in the identification of 49 distinct events (Fig. 2B). The CCLME dominated event counts, with only 9 of the 49 regionally aggregated events occurring in the Gulf of Alaska and either the Northern or Southern Bering Sea. However, survey coverage was considerably higher in the CCLME, such that event detection was much higher. Although event counts per year were higher from 2005 onwards (Fig. 2B), this is largely a reflection of expansion of survey effort (i.e. Fig. 2A). Furthermore, prior to 2001, survey coverage in the CCLME was limited to central California (Beach Watch and BeachCOMBERS; Fig. 1), likely limiting event detection and giving rise to the sparsity of events before the early 2000s (Fig. 2B). Only 2 events were identified in the Salish Sea (2007 and 2016), with the 2016 event extending to the northern outer coast of Washington (Fig. 2A).

Category 4 events, corresponding to the highest carcass encounter rates, rarely occurred (n = 8), with 5 occurring between 2014 and 2019 (Fig. 2B–D). These events were dominated by alcids between 2014 (Cassin's auklets *Ptychoramphus aleuticus*) and 2019 (common murres), and by procellarriids prior to 2014 (northern fulmars *Fulmarus glacialis* in 2003) and from 2019 onwards (short-tailed shearwaters *Ardenna tenuirostris*; Table 2). The one exception was a 2009 mortality event that primarily affected scoters *Melanitta* sp. (Table 2). Events with the highest encounter rates did not necessarily coincide with those that were extensive in space (Table 2). Mortality events spanning more than 500 km were identified in 2005 (murres), 2010 (fulmars), and 2012 (puffins, primarily rhinoceros auklets *Cerorhinca monocerata*), but these were all associated with relatively lower average encounter rates (<10 birds km^{-1}; Table 2). Collectively, mortality events prior to 2014 were predominantly either spatially extensive but relatively low average encounter rate (2005, 2010, 2012) or high average encounter rate but more localized (2009; Table 2). Only one high encounter rate, large-extent event was identified prior to 2014 (2003), whereas 4 were identified from 2014–2019 (Table 2). However, categorization of the 1997–1998 mortality event in the CCLME and the 2007 mortality event in the Southern Bering Sea (Table 2) as either large-scale and/or intense is uncertain given that they occurred when survey coverage was relatively lower in these regions.

The lack of coverage in Alaska prior to 2006 combined with sparse coverage relative to the CCLME

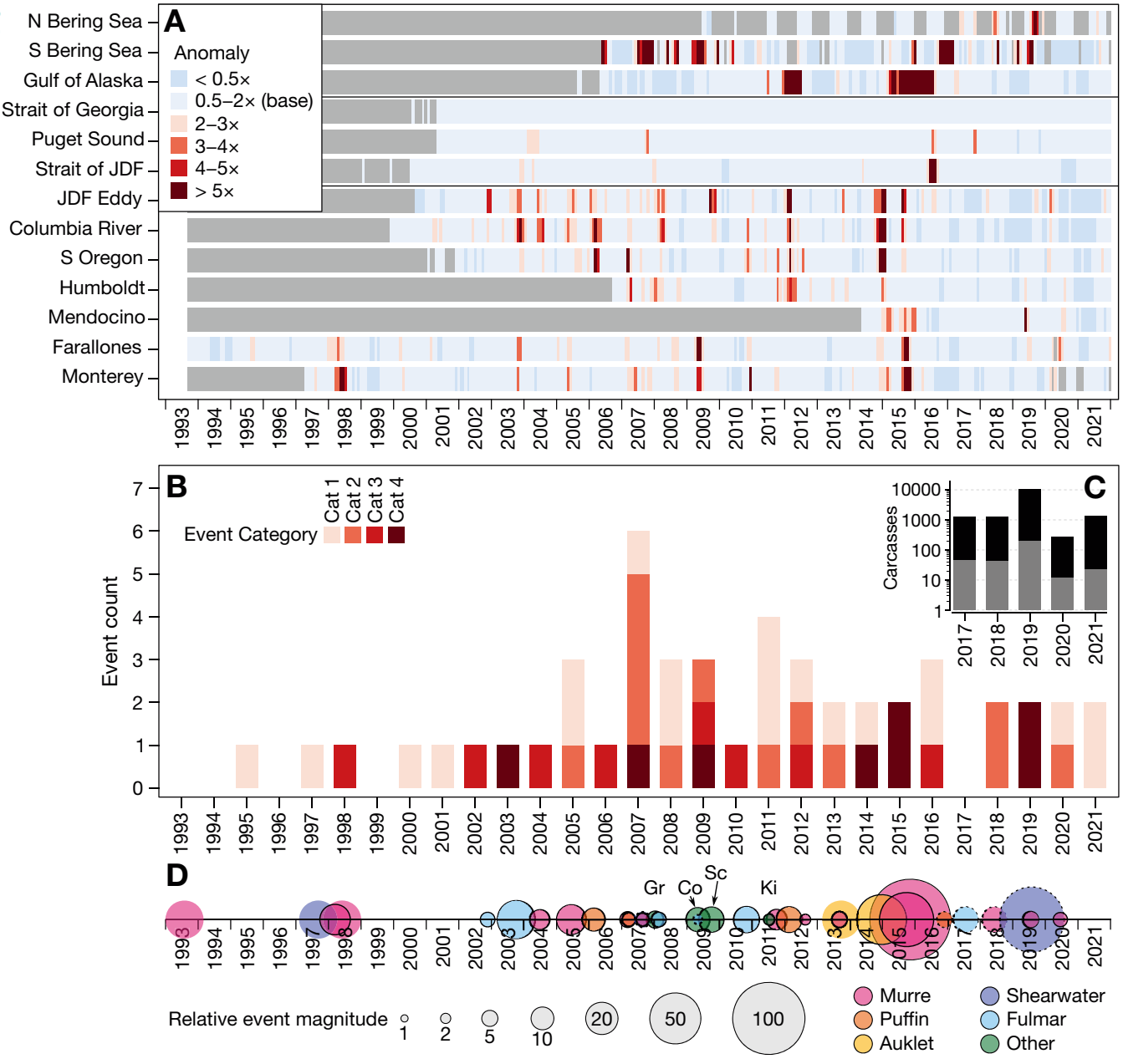

Fig. 2. Regional patterns of carcass encounter rate (carcasses km^{-1}) anomaly relative to seasonal baselines, and summarized information regarding mortality event occurrence. (A) Region-specific encounter rate anomalies, defined as the multiplicative difference between observed carcass encounter rate and seasonal baselines, from 1993–2021. Grey bars: beached bird monitoring data were unavailable. (B) Aggregated event counts by year, shown according to event onset year and color-coded according to encounter rate category (see Table 1). (C) Opportunistic reports of seabird mortality in the Southern and Northern Bering Seas, shown in annual-summarized form as cumulative carcass count (black) and mean carcass count per report (grey). Given the nature of opportunistic reporting, these data are not effort-standardized. (D) Graphical representation of mortality event occurrence through time (circle size is scaled to relative event magnitude), calculated as the product of event-averaged encounter rate, duration, and spatial extent (calculated values are equivalent to values shown in D × 10 000). Events are color-coded according to dominant taxonomic group (Gr: grebe *Aechmophorus* spp.; Co: cormorants *Urile* spp.; Sc: scoters *Melanitta* spp.; Ki: kittiwakes *Rissa* spp.). For events primarily documented in opportunistic reports (dashed circles), spatial extent was approximately estimated (500 km in 2017–2018, 800 km in 2019, 100 km at other times). Major events documented in the literature (1993: Piatt & Van Pelt 1997; 1997: Baduini et al. 2001; 1998: Piatt et al. 1999; 2013: Bodenstein et al. 2015) but not captured in our analyses are also shown (no outline) as equal-sized circles, as equivalent magnitude measures were not comparable among published events. Events documented via opportunistic reports and published literature in (D) are shown for illustration purposes only and are not included in further statistical analyses

Table 2. Large-scale and/or high encounter rate marine bird mortality event characteristics and taxonomic composition. Events are aggregated and represent those that were either in the highest encounter rate category or extended over more than 500 km of coastline (**bold**). Summaries for events in the Northern and Southern Bering Sea that were primarily documented by opportunistic reports are given for years where the opportunistic count exceeded 1000 birds. Max encounter rates represent the peak encounter rate observed in a particular region and month throughout the mortality event duration. Counts and encounter rates represent all marine bird carcass finds within event bounds. CC: California Current Large Marine Ecosystem (LME); GA: Gulf of Alaska LME; SBS: Southern Bering Sea LME; NBS: Northern Bering Sea LME

LME	Timing	Encounter rate		Extent	Magn.	Composition			
		Cat.	Mean (max.)	(km)	(×1000)	Count	Primary	Secondary	Tertiary
CC[a]	Dec–Jul 1997–1998	3	3.0 (5.9)	**348**	**178**	2996	Murre (34%)	Scoter (12%)	Shearwater (11%)
CC	Aug–Feb 2003–2004	4	**4.2 (13.2)**	**798**	**279**	3776	Fulmar (79%)	Murre (7%)	Gull (6%)
CC	Apr–Oct 2005	3	2.5 (5.7)	**755**	**170**	2328	Murre (48%)	Cormorant (24%)	Gull (15%)
SBS[b]	Jun–Nov 2007	4	**2.2 (9.0)**			116	Shearwater (53%)	Fulmar (16%)	Murre (13%)
CC	Sep–Dec 2009	4	**5.4 (10.0)**	320	**121**	2612	Scoter (36%)	Murre (22%)	Fulmar (22%)
CC	Oct–Dec 2010	3	5.1 (7.6)	**524**	**132**	3379	Fulmar (76%)	Gull (6%)	Murre (5%)
CC	Jan–May 2012	3	2.0 (4.3)	**641**	**127**	1631	Puffin (53%)	Grebe (12%)	Murre (9%)
CC	Oct–Mar 2014–2015	4	**5.2 (28.1)**	**813**	**478**	13238	Auklet (66%)	Murre (11%)	Fulmar (6%)
CC	Jul–Jan 2015–2016	4	**6.8 (14.3)**	**810**	**562**	11312	Murre (76%)	Cormorant (8%)	Gull (5%)
GA	May–Mar 2015–2016	4	**5.0 (49.5)**	**850**	**1924**	5109	Murre (97%)	Gull (1%)	Auklet (1%)
CC	May–Oct 2019	4	**3.4 (9.3)**	311	52	1322	Murre (75%)	Cormorant (5%)	Puffin (4%)
SBS[c]	Jun–Oct 2019	4	**10.3 (41.2)**			960	Shearwater (91%)	Kittiwake (3%)	Murre (2%)
Opportunistic reports (years with >1000 birds reported)									
NBS	Jun–Sep 2017			~600		1177	Fulmar (44%)	Shearwater (30%)	Murre (15%)
NBS	May–Jul 2018			~500		1232	Murre (92%)	Shearwater (3%)	Fulmar (1%)
SBS-NBS	Jun–Oct 2019			~800		10507	Shearwater (95%)	Murre (2%)	Kittiwake (1%)
NBS	Jun–Sep 2021			~300		1318	Shearwater (60%)	Murre (27%)	Kittiwake (7%)

[a]This event occurred prior to widespread monitoring throughout the CCLME, and therefore the event extent and magnitude are likely underestimates
[b]This event occurred early after monitoring commenced in the Southern Bering Sea, and few sites were monitored at that time
[c]This event is also noted in the Opportunistic reports category

certainly biased our results towards the south. Despite the sparsity of regular survey coverage (i.e. Fig. 1), our primary analyses indicated mortality events in the Southern Bering Sea in 2007 and 2016 and throughout the Southern and Northern Bering Sea in 2018 and 2019. However, opportunistic reports were also suggestive of mortality events in the Northern Bering Sea in 2017 and 2021 (Fig. 2C), primarily concentrated in the Bering Strait, north of St. Lawrence Island (Fig. S15 in Supplement 3). The total number of carcasses reported opportunistically along with the mean counts per report suggest similar-magnitude mortality events in 2017 (approximate total carcass count, N ≈ 1200), 2018 (N ≈ 1200), and 2021 (N ≈ 1300), in addition to the much larger and more expansive (Southern and Northern Bering Sea) event in 2019 (N ≈ 10 000; Fig. 2C). Opportunistic reports were also made in 2020; however, the total number of carcasses reported (N ≈ 250) and the average count per report were seemingly not reflective of unusually high mortality in that year (Fig. 2C).

3.2. Event characteristic analyses

Aggregated event (n = 49) statistics varied considerably among events, with each individual characteristic spanning one or more orders of magnitude (Fig. 3). Relative to long-term baselines of carcass encounter rate, 57% of all regionally aggregated events had encounter rate anomalies 2–3 times above seasonal baselines, with only 6 events exceeding 5 times the baseline (Fig. 3A). However, all of these events were from LMEs in Alaska, where baseline encounter rates are very low at certain times of year, potentially inflating these measures. Duration and spatial extent were also skewed towards shorter, smaller events, with only 14% of all events lasting longer than 4 mo and 16% (n = 43; excluding Southern and Northern Bering Sea events where extent calculations were not performed) spanning more than 500 km (Fig. 3).

Aggregated event characteristics displayed no consistent linear trend through time (Table S8 in

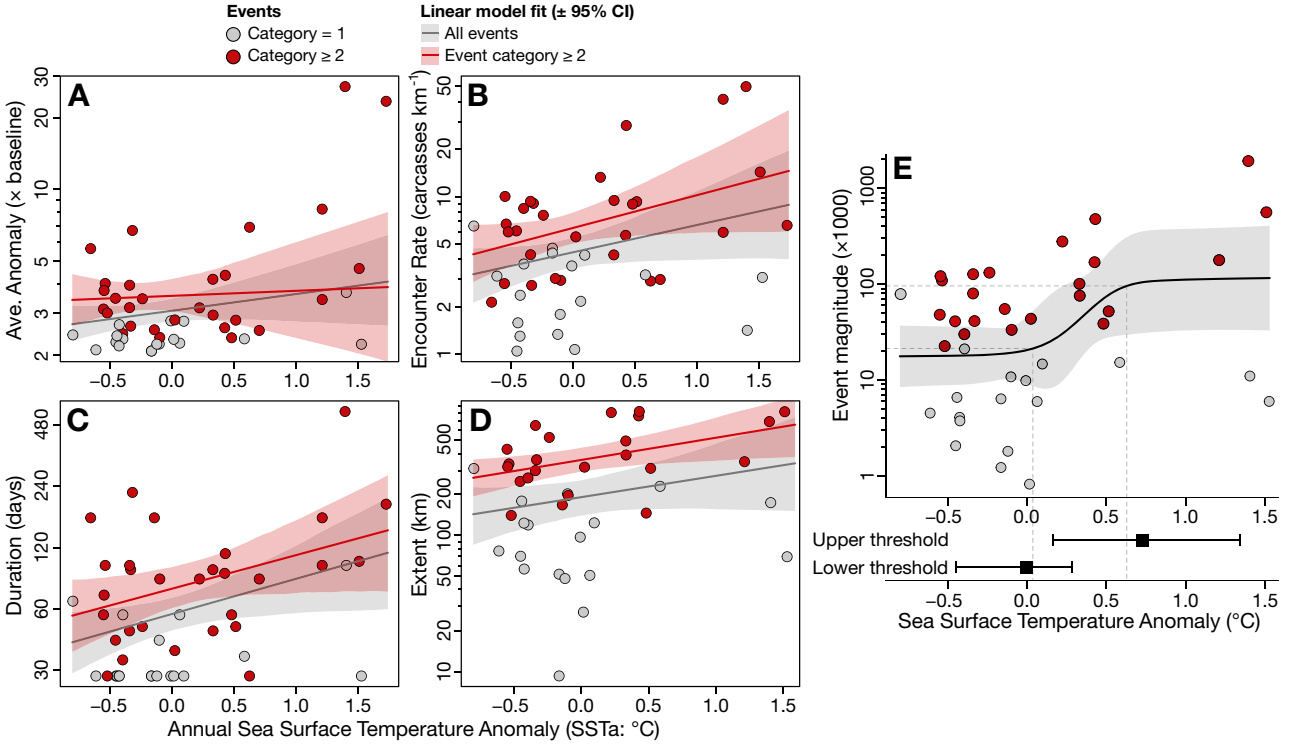

Fig. 3. Mortality event characteristics as a function of annual (year before event onset) sea surface temperature anomaly (SSTa): (A) average anomaly, defined as the multiplicative difference between observed and expected baseline encounter rate; (B) average carcass encounter rate per km of beach; (C) event duration, calculated as the number of days where encounter rate anomaly was above 2×; (D) event extent, estimated as the km of shoreline with elevated beached bird encounter rate; and (E) event magnitude, calculated as the product of average encounter rate, duration, and extent as a relative measure of total deposition. Response variables are aggregated event characteristics identified across the 4 large marine ecosystems we examined, calculated by either averaging (anomaly, encounter rate, duration) or summing (extent, magnitude) constituent regional mortality event data to ensure that distinct events are uniquely represented. In (A–E), events are delineated by event encounter rate category. Lines and shaded polygons in (A–D) indicate fitted linear regression models (mean and 95% confidence interval) fitted to all events (grey), and limited to Category 2–4 events (red). In (E), lines (mean) and shaded regions (±2 SE) show a shape-constrained (monotonic increase) generalized additive model fit. Dashed lines: lower and upper function bounds, defined as the minimum function value + 10/90% of the function range, respectively, and the corresponding thresholds calculated as the SSTa values where the fitted function crosses those bounds. Mean and 95% confidence intervals of threshold SSTa values are shown under (E)

Supplement 5). For the majority of characteristics, models with time as a predictor had higher AICc values than corresponding null models and bootstrapped 95% confidence intervals of trend estimates overlapped with zero (Table S8 in Supplement 5). We found moderate to weak support for linearly increasing trends of encounter rate anomaly (trend = 0.021, 95% CI = [0.003, 0.039], ΔAICc = 5.4 compared to null) and event magnitude (trend = 0.136, 95% CI = [−0.028, 0.322], ΔAICc = 0.3), albeit the latter only when excluding the lowest event category (Table S8 in Supplement 5). However, these results were driven almost exclusively by events in 2015–2016, and trend estimates were not robust to their removal. In summary, there was weak-to-no evidence that either individual event characteristics or cumulative event magnitude increased (linearly) throughout the study period.

However, we found that aggregated mortality event characteristics were correlated with SSTa averaged over the year prior to event onset date, tending toward more extreme events following periods of elevated SST (Fig. 3). Not all mortality events, however, were associated with warmer conditions. Year-averaged SSTa varied widely among mortality events, ranging from cooler (SSTa = −0.8°C) to considerably warmer (SSTa = +1.7°C) than normal conditions (Fig. 3). Events following warm (SSTa > 0) conditions included a greater proportion of higher encounter rate category (2–4) events (cool: 54%, n = 27; warm: 71%, n = 22), and averaged longer durations (cool: mean = 65 d; warm: mean = 90 d), and

larger spatial extents (cool: mean = 233 km; warm: mean = 408 km) (Fig. 3).

With the exception of encounter rate anomaly, models of event characteristics with SSTa as the sole predictor were supported over null models based on AICc (Table 3). For event extent and average carcass encounter rate, evidence in favor of the SSTa model over the null model varied from weak to moderate (ΔAICc < 2; Table 3). However, there was relatively stronger evidence of SSTa effects for event duration and magnitude response variables (ΔAICc > 2; Table 3). Despite that, SSTa only explained a small proportion of event characteristic variation (3–15%; Table 3), and while SSTa trend coefficient point estimates were uniformly positive, confidence intervals overlapped with zero for all but event duration (Table 3). However, excluding Category 1 events strengthened SSTa relationships for extent, duration, and event magnitude (Table 3).

The inclusion of season as a categorical predictor was only supported for models of average carcass encounter rate and for event duration when Category 1 events were excluded (Table 3). Autumn had the highest carcass encounter rates compared to other seasons, possibly resulting from elevated post-breeding mortality of juveniles and adults, whereas event durations were more prolonged in winter, and shorter during summer (Table S9 in Supplement 5).

Non-linear models of event magnitude as a function of prior-year averaged SSTa revealed a sigmoidal (step-function) relationship for both shape-constrained (SC-GAM: monotonically increasing function) and unconstrained GAMs (Fig. 3E). Both model types were supported over the null model (lower AICc) and were functionally equivalent in shape. Given that, and along with the lower AICc value of the SC-GAM compared to the unconstrained GAM (ΔAICc = 1; Table 3), we based all

Table 3. Model statistics and trend estimates from models fitted to event characteristics as a function of year-averaged sea surface temperature anomaly (SSTa). Model statistics for non-linear generalized additive models of event magnitude are presented for unconstrained (GAM) and shape-constrained (SC-GAM) models. Mean trend estimates of SSTa coefficients are given for linear models, along with their bootstrapped 95% confidence intervals. AICc: Akaike's information criterion adjusted for small sample size

Response variable	Model	All events			Event Category: 2–4		
		AICc	R^2	Trend estimate (95% CI)	AICc	R^2	Trend estimate (95% CI)
Average event anomaly	ln(y) ~ 1	51.6			36.4		
	ln(y) ~ SSTa	52.5	3	0.16 (–0.09, 0.38)	39.0	0	0.03 (–0.35, 0.38)
	ln(y) ~ season	58.6	1		43.2	7	
	ln(y) ~ SSTa + season	60.0	4	0.15 (–0.18, 0.39)	46.6	7	–0.07 (–0.85, 1.00)
Average carcass encounter rate	ln(y) ~ 1	119.6			68.7		
	ln(y) ~ SSTa	118.4	7	0.41 (–0.01, 0.90)	66.3	16	0.48 (0.02, 0.97)
	ln(y) ~ season	110.2	30		58.2	49	
	ln(y) ~ SSTa + season	109.5	35	0.38 (–0.05, 0.84)	59.6	52	0.32 (–0.15, 0.80)
Duration[a]	ln(y) ~ 1	104.7			63.4		
	ln(y) ~ SSTa	99.7	15	0.40 (0.02, 0.74)	60.8	16	0.37 (–0.03, 0.71)
	ln(y) ~ season	111.5	1		65.8	18	
	ln(y) ~ SSTa + season	105.3	18	0.45 (0.05, 0.85)	59.9	40	0.49 (0.06, 0.82)
Extent[a]	ln(y) ~ 1	120.2			40.7		
	ln(y) ~ SSTa	120.6	5	0.37 (–0.10, 0.78)	38.7	18	0.37 (0.04, 0.68)
	ln(y) ~ season	126.7	2		48.9	3	
	ln(y) ~ SSTa + season	126.9	8	0.40 (–0.13, 0.87)	48.0	21	0.37 (–0.04, 0.76)
Event magnitude[a]	ln(y) ~ 1	165.6			72.2		
	ln(y) ~ SSTa	163.5	10	0.90 (–0.10, 1.87)	60.5	46	1.16 (0.44, 1.75)
	ln(y) ~ season	170.8	5		80.7	2	
	ln(y) ~ SSTa + season	166.6	20	1.11 (–0.15, 2.21)	67.9	52	1.24 (0.33, 1.92)
	GAM: ln(y) ~ s(SSTa)	163.9	19				
	SC-GAM: ln(y) ~ s(SSTa)[b]	162.9	16				

[a]These models did not contain the variance function as there was no indication of heteroscedasticity of model residuals
[b]Presented model statistics are for the SC-GAM with a monotonically increasing functional form. The equivalent model, specified to include a monotonically decreasing function, was equal to the null model, as no decreasing relationship was plausible given the data

further results on the SC-GAM. For colder than normal conditions (i.e. SSTa < 0°C), the model estimated a near constant and relatively lower average event magnitude, indicating no impact of ocean temperature on marine bird mortality event magnitude within this temperature range. However, above SSTa = 0°C (lower threshold estimate, 95% CI = [−0.45, 0.28]°C), the model indicated an increase in mean event magnitude, reaching a plateau at SSTa = 0.73°C (upper threshold, 95% CI = [0.17, 1.34]°C; Fig. 3E). Furthermore, between SSTa = 0°C and SSTa = +1°C, the model estimated a mean difference of 1.67 (95% CI = [0.14, 3.28]) in log-magnitude. This suggests that mortality event magnitudes averaged 5.3 times higher (95% CI = [1.1, 26.6]) when preceded by prolonged warming above +1°C than when following near climatological average (i.e. SSTa ~ 0°C) conditions.

3.3. MHW association analyses

From 1993 to 2021, MHWs, operationally defined as SST assessed at the LME scale exceeding the 90th climatological percentile for a minimum of 6 consecutive days, occurred in clusters of years (Fig. 4A). During this period, MHW days occurred 13.3% of the time throughout the CCLME but were more common to

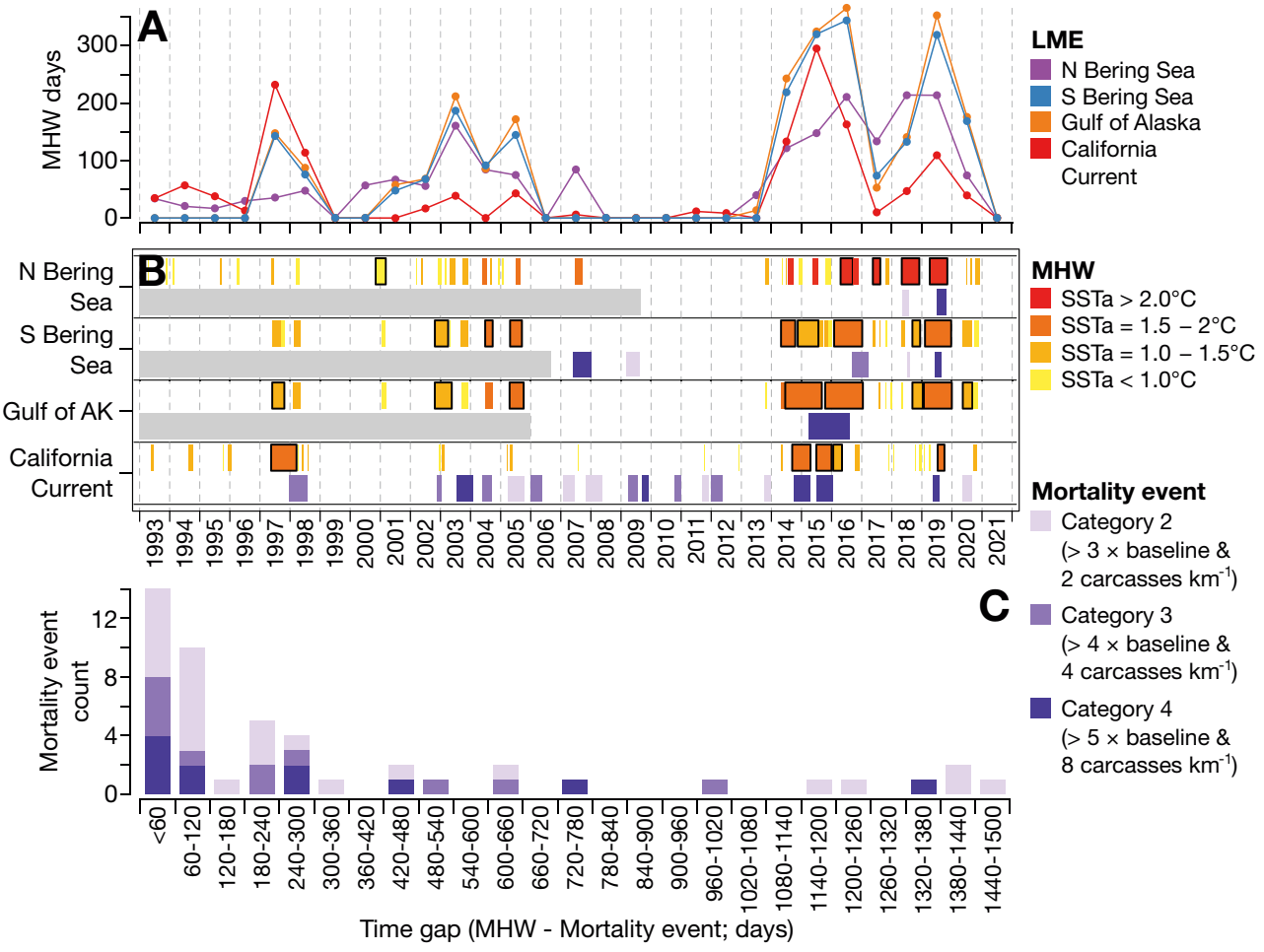

Fig. 4. Marine heatwave and mortality event association patterns. (A) Number of marine heatwave (MHW) days in the California Current, Gulf of Alaska, Southern Bering Sea, and Northern Bering Sea large marine ecosystems (LME). Marine heatwaves were defined according to sea surface temperature (SST) (region-average within 100 km of shore) in excess of the 90th percentile of SST based on the 1981–2010 climatology. (B) MHW (top row) and mortality event (bottom row) occurrence plotted through time for each LME, where MHWs are coded according to average SST anomaly (SSTa), and mortality events are delineated by event encounter rate category (key: bottom right). MHWs lasting longer than 90 d are surrounded by a thick black border; grey rectangles: periods during which monitoring data were unavailable. (C) Frequency distribution (60 d bin size) of the observed time gap between encounter rate Category 2–4 mortality events (key: bottom right) and the most recent MHW in the corresponding LME

the north (Gulf of Alaska: 23.6%; Southern Bering Sea: 22.1%; Northern Bering Sea: 18.2%; Fig. 4A). Several MHW events were prolonged, lasting months to years, specifically in 1997–1998, 2003–2005, and 2014–2020 (Fig. 4B).

While multiple mortality events were observed following MHWs (Fig. 4B), they also occurred between MHW episodes (Fig. 4B). However, assessed at the regional scale, the time between mortality events and the most recent MHW was skewed, with half (24 of the 48 Category 2–4 mortality events) occurring within 120 d of a MHW, rising to almost three-quarters (35 of 48) occurring within 1 yr (Fig. 4C). Permutation testing via random re-assortment of mortality events at the regional level suggested that, while not a necessary requirement, mortality events occur more frequently following MHWs, suggestive of an association between these 2 phenomena. There were more regional mortality events within 1 yr of a MHW (observed: 35, 95% range from permutations = [21, 36], p = 0.068), as well as a shorter mean time gap (observed: 340 d, 95% range = [317, 679], p = 0.044) between MHWs and mortality events than expected by chance. This pattern was also true when limiting permutation testing to only the more extreme regional mortality events (Category 3–4; Table S10 in Supplement 6).

3.4. Post MHW impacts on beached bird abundance

To explore potential similarities in ecosystem response to prolonged MHWs, we examined 3 focal MHWs (1997–1998 ENSO, 2014–2016 NE Pacific MHW, 2019 ENSO) within the central California Current (Farallones and Monterey regions) where our data set is most comprehensive. The progression of regional encounter rate anomalies, aligned relative to MHW onset date, bore strong similarities in both the timing of mortality event occurrence and in the following period of depressed carcass encounter rates (negative anomaly values; Fig. 5). Regional mortality events appeared to cluster into 2 distinct time windows following MHW onset: approximately 1–6 mo later, with a second mode at approximately

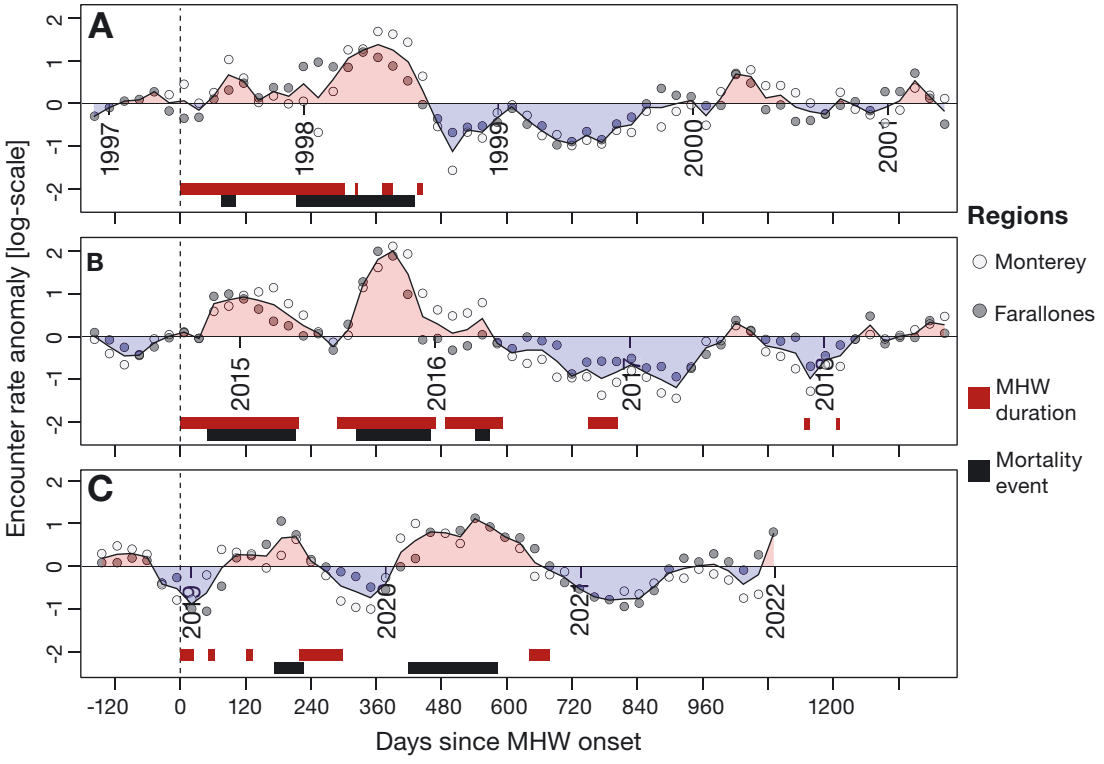

Fig. 5. Anomaly in beached bird encounter rate (carcasses km^{-1}) in the central California Current large marine ecosystem following major marine heatwave (MHW) events in (A) 1997–1998, (B) 2014–2015, and (C) 2019 plotted according to time since MHW onset. Plotted points are the model-derived anomaly values for each 28 d time window estimated for the Monterey and Farallones regions; line and shaded regions: anomaly averaged across these 2 regions. All panels are aligned according to MHW onset date (vertical dashed line); dark red and black polygons: MHW and mortality event durations, respectively

10–16 mo (Fig. 5). Following that, an approximate 16 mo period (~450–500 d) of depressed carcass encounter rates was also consistently observed (Fig. 5). Although the magnitude and exact timing of mortality events and the subsequent depression differed among the 3 MHW episodes, the emergent pattern and durations appeared consistent among the 3 large-scale MHWs examined (Fig. 5). These comparisons suggest that, at least within the CCLME, ecosystem response to a prolonged MHW may include a cascade of marine bird mortality events followed by subsequent reductions in beaching rates collectively lasting nearly 3 yr.

4. DISCUSSION

Our analysis suggests that low-level marine bird mortality events, indicated by significant elevations in carcass beaching rate, are fairly common (Fig. 2A). However, mass mortality events, with order-of-magnitude increases in carcass encounter rate spanning multiple months and regions (i.e. Jones et al. 2018, Piatt et al. 2020; Fig. 2) are rare. We demonstrate that these extreme events are more likely following MHWs (Fig. 4), and that event magnitudes are on average 5 times larger following sustained (annual) SSTs of 0.5–1°C above climatology (1981–2010; Fig. 3E). Our results also suggest a systemic response to MHWs in the CCLME (Fig. 5), consisting of repeated mortality event occurrences followed by an extended period of depressed carcass deposition; a pattern that seemingly spans 3 yr post-MHW.

Our study is also the first to present a synoptic view of the mortality events that occurred in the Northeast Pacific from 2014 through 2019, starting in the CCLME in 2014 (Jones et al. 2018), propagating northwards through the Gulf of Alaska in 2015–2016 (Piatt et al. 2020) and culminating in a succession of events in the Southern and Northern Bering Sea in 2016 through 2019 (Jones et al. 2019, Romano et al. 2020, Van Hemert et al. 2020, Will et al. 2020a; Fig. 2). We believe that this sequence of mortality events is unprecedented in terms of their frequency, extent, and magnitude. Furthermore, these events coincided with multiple ocean-heating phenomena; specifically, the prolonged MHW (Di Lorenzo & Mantua 2016, Lim et al. 2017) of 2014–2016 and transition to a warm stanza accompanied by massive retraction of sea ice in the Bering and Chukchi Seas (Stabeno & Bell 2019). The sequence of mass mortality events from 2014–2019 likely resulted in excess mortality of several million birds.

4.1. Methodological considerations

Prior to 2009 in the Northern Bering Sea and 2006 elsewhere in Alaska, we have no effort-controlled data for Alaska and rely on published accounts (i.e. Piatt & Van Pelt 1997, Baduini et al. 2001) to infer event occurrence (Fig. 2). A similar temporal bias also exists prior to 2001 within the CCLME, with effort-controlled data south of Mendocino only (Fig. 1). Consequently, interpretation of mortality event occurrence and/or scale prior to these epochs should be treated with caution. In particular, the spatial scale of the 1997–1998 mortality event in the CCLME was likely underestimated due to the lack of concurrent effort-controlled monitoring outside central California. Because the 1997–1998 ENSO-driven event coincided with mortality of shearwaters in the Southern Bering Sea (Baduini et al. 2001) as well as common murres in the Gulf of Alaska (Piatt et al. 1999), this may well have been a multi-ecosystem mortality event sequence similar to those observed following the 2014–2016 Northeast Pacific MHW, albeit of a lower magnitude.

Even with the inclusion of opportunistic data from the Northern Bering Sea (Fig. S15 in Supplement 3), lower coverage in this region inhibited our ability to identify mortality events other than those that were large-scale and/or coincident with beached bird monitoring (e.g. the localized puffin mortality event documented on St Paul Island; Jones et al. 2019). Given the temporal extent, geographic breadth, and grain of survey coverage throughout the CCLME relative to Alaska, many more localized events were detected in the CCLME, potentially biasing our results towards over-representing the former. To some degree, regionalization of analyses into approximately 200 km segments of coastline within the CCLME addressed this issue, as very local events (~10s of km) would not register according to our event criteria.

While data gaps likely induced spatial biases and differences in spatial scale, we do not believe that they impact the inferred relationships between event occurrence or characteristics and SSTs. We maintain that our main results — the occurrence of an unprecedented sequence of mass mortality events between 2014 and 2019 and the relationships with SSTa and MHWs — are robust to these data gaps.

4.2. Population impact

Marine bird populations can withstand significant annual mortality without declining (Frederiksen et al.

2008), especially when elevated mortality is limited to pre-reproductive age classes and does not persist over multiple years (Tuck et al. 2015, Johns et al. 2022). The degree to which mass beaching events are representative of increased mortality versus changes in distribution (e.g. Jones et al. 2018) is debatable, although both are a necessary requirement for mortality events with carcass encounter rates that are orders of magnitude above normal. Furthermore, whether mortality observed during any large mortality event is additive versus compensatory is also likely to fall along a continuum. Thus, while sudden, distinct episodes of marine bird mortality can be highly visible, the associated population impacts may in some instances be offset by reduced mortality overall (Frederiksen et al. 2008).

For most marine bird populations, assessing population impacts is only possible on the breeding colonies. Even in high single-event mortality situations, changes in colony size may be obscured by surviving older pre-reproductives and adult age classes otherwise excluded from securing breeding positions (i.e. the floating population) 'filling up' newly vacated space (Johns et al. 2022). Despite this obscuring factor, there is evidence that several of the mass mortality events described herein depressed breeding population size and subsequent vital rates.

Following the Cassin's auklet mortality event in the winter of 2014–2015, Jones et al. (2018) reported a 15% decline in burrow occupancy rates on Triangle Island, British Columbia, the largest Cassin's auklet colony worldwide. To the south on Southeast Farallon Island, California, Johns et al. (2022) estimated that annual apparent survival in 2014 was 51%, down from 80% on average. While burrow occupancy in 2015 (following the mortality event) was not depressed, auklets shifted their breeding strategy from 'record high' double-clutching (40–80%) prior to the event (2010–2014) to less than 10% of pairs engaging in this strategy over the following years (2015–2019). These authors hypothesized that higher than average productivity from 2010–2014 likely increased the floating population, which subsequently occupied available burrows following elevated mortality in 2014.

Subsequent to the short-tailed shearwater mass mortality event in the Southern and Northern Bering Sea in 2019, Glencross et al. (2021) reported delayed arrival of adults to Bruny Island in Southeast Tasmania, Australia, and a curtailed 'pre-laying exodus' to the Southern Ocean to forage prior to breeding. Although burrow occupancy was not depressed, breeding success was low (33% compared to 50–75% typically) and nest abandonment was widespread. These authors suggest that foraging stress in the Bering Sea forced adults farther north and left survivors in poorer body condition facing a longer migration.

Finally, and most seriously, leading into and following the extreme die-off of common murres in Alaska in 2015–2016, Piatt et al. (2020) reported severe depression of reproductive success throughout monitored colonies in Alaska (n = 13), with all colonies failing (i.e. colony abandonment) at least once during 2015–2017 and multi-year failures at 8 colonies. Indeed, total breeding failures continued into 2019 at some colonies in the Gulf of Alaska (Schoen et al. 2022, this Theme Section). These changes were concurrent with, or subsequent to, the loss of upwards of one-quarter of all breeders in Alaska during the mortality event, constituting at least 1 million individuals. In 2018, a second mortality event of common murres also occurred, centered in the Northern Bering Sea (Romano et al. 2020). We suggest that when multiple mass mortality events involve a single species, even the most robust populations can become threatened.

4.3. Mechanisms

Our work reinforces studies worldwide indicating that a warmer ocean will be different in terms of community composition (Brown et al. 2010, Gurgel et al. 2020) and ecosystem function (Smale et al. 2019, Smith et al. 2023). The mechanisms by which those changes occur are diverse and complex (Gissi et al. 2021), including both direct and indirect effects (e.g. trophic-mediated changes to grazing pressure; Batten et al. 2022). The range of mortality events contained in this synthesis are indicative of the myriad of mechanistic pathways ending in sudden and dramatic, albeit short-term, increases in marine bird mortality. Bottom-up trophic factors appear to include lower productivity (Beardall et al. 2009, Gao et al. 2021), in some cases associated with phenological shifts in seasonal upwelling (e.g. Parrish et al. 2007), and alterations to zooplankton (e.g. copepods, euphausiids) community composition (Hipfner et al. 2020, Batten et al. 2022), with a concurrent shift in size distribution towards smaller, relatively energy-poor species (Arimitsu et al. 2021, Killeen et al. 2022). However, a host of non-trophic impacts have also been associated with warmer Northeast Pacific and Bering Sea waters, including increases in disease (Bodenstein et al. 2015, Knowles et al. 2019) and the occur-

rence of toxic (Ryan et al. 2017, Van Hemert et al. 2020) and non-toxic harmful algal blooms (Jessup et al. 2009, Jones et al. 2017).

It is worth noting that beached bird abundance, although certainly an indicator of increased mortality, is not linearly related to population vital rates. This is because a bird that becomes moribund or dies at sea will be scavenged or sink before washing ashore unless the body is already within a narrow strip of coastal ocean (Wiese 2003, O'Hara & Morgan 2006). Therefore, sudden and dramatic increases in carcass deposition rate imply that victims had already made decisions to stay within, or migrate to, the coastal zone. Given that many of the species experiencing mass mortality events in the Northeast Pacific since 2014 were alcids and/or procellariids (Table 2), which have a distinctly offshore distribution post-breeding (e.g. Hunt 1990, Hatch et al. 2000, 2010, Hedd et al. 2012), one interpretation is that deteriorating offshore conditions drove birds onshore. Following the 2014–2016 Northeast Pacific MHW, changes in forage fish abundance (Santora et al. 2020) and quality (Arimitsu et al. 2021) of nearshore species have been documented, which may have provoked inshore movement (Jones et al. 2018). It remains unknown, however, how or even whether offshore prey fields changed.

Finally, the under-representation in these mortality events of several abundant nearshore marine bird taxa, including larids and phalacrocorids, suggests that ecosystem impacts that precipitate mortality events are not uniformly experienced among marine bird taxa. Some taxonomic groups may be relatively buffered against ecosystem shifts due to a combination of foraging behavior (Osborne et al. 2020), metabolic adaptations (Burke & Montevecchi 2018), and/or dietary breadth (Baltz & Morejohn 1977, Will et al. 2020b, Tate et al. 2021). For instance, larids (Blight et al. 2015) and phalacrocorids (Watanuki et al. 2004, Kotzerka et al. 2011) are generalist foragers, which may buffer them against losses of individual prey sources. Will et al. (2020a) found that reductions in the availability of pelagic prey in the Northern Bering Sea from 2016–2019 resulted in higher nutritional stress in common murres relative to congeneric thick-billed murres *Uria lomvia*, which they attributed to a more diverse diet and benthic foraging habits in the latter species. In summary, different rates of mortality among seabird species may be related to their greater ability to exploit alternate prey than the pelagic species that were severely impacted during recent MHWs (Arimitsu et al. 2021).

4.4. Indicators of change

Several studies have suggested that the North Pacific will be less productive as it continues to warm (Ainsworth et al. 2011, Bryndum-Buchholz et al. 2019), resulting in a lower carrying capacity for epipelagic upper trophics (Woodworth-Jefcoats et al. 2017), including marine birds. Piatt et al. (2020) proposed that ocean warming creates an 'ectothermic vise' for marine birds. Warming reduces bottom-up production but increases metabolism and food demands of forage fish, thereby reducing their size and energy content. Simultaneously, warming also increases the metabolism and food demands of large predatory fish (Holsman & Aydin 2015), increasing top-down competition for forage fish. At the broadest scale, our data suggest that recent warming in the Northeast Pacific has provoked an increase in the frequency and magnitude of marine bird mass mortality events. However, we hypothesize that it is not the absolute value of SST, but rather the abrupt increase in ocean temperature (i.e. following MHW onset, Fig. 5) with concomitant bottom-up impacts on trophic dynamics that provokes a mortality event (Piatt et al. 2020). In some instances, these changes may occur over time scales of weeks (Montevecchi et al. 2021).

Our models hint that following a prolonged MHW, marine bird mortality events spaced at 1–6 mo, and again at 10–16 mo, preceded a relatively quiescent period of less-than-normal deposition in the CCLME. While we are confident that mortality events are an indication of excess mortality in the short term, there are multiple competing hypotheses for lower deposition over subsequent months to years. These include depressed breeding productivity and colony attendance resulting in reduced carcass deposition via the production of fewer fledglings and/or altered at-sea distribution, compensatory mortality in adult birds, and/or reductions in population size before affected populations adjust back towards carrying capacity. Several regions in the CCLME appear to display long-term reductions in carcass encounter rate that did not fully recover following the 2014–2016 Northeast Pacific MHW (i.e. Columbia River [Fig. S7] and Juan de Fuca Eddy [Fig. S8 in Supplement 2]), potentially indicative of population decline. As MHW frequency increases (Benedetti-Cecchi 2021), we posit that the chance of compounding effects will increase as marine bird populations fail to fully recover between MHW episodes.

4.5. Conclusions

While marine bird mortality events are one manifestation of ecosystem change, there is still much uncertainty regarding causal mechanisms and the degree of population impact. Nevertheless, the occurrence of multiple sequential mass mortality events in the Northeast Pacific and Bering Sea between 2014 and 2019 represents an order of magnitude increase in their frequency, given the occurrence of 1–2 events of a similar magnitude in the 20 yr prior (Table 2). Given that these events likely include some of the largest marine bird mortality events that have ever been documented, and that each was associated with changes in population vital rates, it is likely that the abundance of North Pacific marine birds was reduced by millions of birds as a result. Thus, the question now becomes whether carrying capacities will be absolutely lower given chronic forcing towards warmer conditions as a baseline rather than an anomaly (Benedetti-Cecchi 2021); and secondarily, whether the frequency of marine bird mortality events will slow should the rate of warming decelerate — an admittedly optimistic view given the continued increase in greenhouse gas emissions globally.

Acknowledgements. A data set of this scale would be impossible to collect and maintain without the efforts of thousands of volunteer participants and interns over 2 decades and across 4 citizen-science programs: COASST (University of Washington), BeachCOMBERS (Moss Landing Marine Laboratories), Beach Watch (Greater Farallones Association), and BC Beached Bird Survey (Birds Canada). Special mention to Mireya Bejarano and Kathya Argueta (US Fish and Wildlife Service, USFWS) for their efforts to prepare the BeachCOMBERS data set for these analyses. Funding for the Beach Watch project was provided by NOAA–Greater Farallones National Marine Sanctuary and Greater Farallones Association. We thank the National Parks Service in Alaska for their contributions to COASST annual data sets, with special thanks to contributors David Payer, Letty Hughes, Raime Fronstin, Mary Hake, and Pam Sousanes for their support of seabird surveys in the Arctic parks. Similar thanks go to annual summer surveyors across remote areas within the Alaska Maritime National Wildlife Refuge. Annual contributions of data and survey development in the Pribilof Islands would not have been possible without the efforts of Pamela Lestenkof, Paul Melovidov, and Aaron Lestenkof of the Ecosystem Conservation Office (ECO). In addition, the opportunistic reports collected in Alaska from 2017–2021 by the USFWS are the result of dedicated efforts by a large group of federal, state, community, and tribal partners, including Brandon Ahmasuk (Kawerak Inc.), Gay Sheffield and Melissa Good (AK Sea Grant), Sarah Schoen (USGS), and Elizabeth Labunski (USFWS). We thank the 3 anonymous reviewers, and content editor (J. Piatt) for taking the time and effort necessary to review and provide constructive comments on this work. The overall quality of the manuscript was much improved following their feedback. The findings and conclusions in this article are those of the author(s) and do not necessarily represent the views of the USFWS.

LITERATURE CITED

Ainley DG, Jones RE, Stallcup R, Long DJ and others (1994) Beached marine birds and mammals of the North American west coast: a revised guide to their census and identification, with supplemental keys to beached sea turtles and sharks, Vol 55. NOAA, Gulf of the Farallones National Marine Sanctuary, San Francisco, CA

Ainsworth CH, Samhouri JF, Busch DS, Cheung WW, Dunne J, Okey TA (2011) Potential impacts of climate change on Northeast Pacific marine foodwebs and fisheries. ICES J Mar Sci 68:1217–1229

Arimitsu ML, Piatt JF, Hatch S, Suryan RM and others (2021) Heatwave-induced synchrony within forage fish portfolio disrupts energy flow to top pelagic predators. Glob Change Biol 27:1859–1878

Avery-Gomm S, O'Hara PD, Kleine L, Bowes V, Wilson LK, Barry KL (2012) Northern fulmars as biological monitors of trends of plastic pollution in the eastern North Pacific. Mar Pollut Bull 64:1776–1781

Baduini CL, Hyrenbach KD, Coyle KO, Pinchuk A, Mendenhall V, Hunt GL Jr (2001) Mass mortality of short-tailed shearwaters in the south-eastern Bering Sea during summer 1997. Fish Oceanogr 10:117–130

Baltz DM, Morejohn GV (1977) Food habits and niche overlap of seabirds wintering on Monterey Bay, California. Auk 94:526–543

Barbeaux SJ, Holsman K, Zador S (2020) Marine heatwave stress test of ecosystem-based fisheries management in the Gulf of Alaska Pacific cod fishery. Front Mar Sci 7:703

Barkhordarian A, Nielsen DM, Baehr J (2022) Recent marine heatwaves in the North Pacific warming pool can be attributed to rising atmospheric levels of greenhouse gases. Commun Earth Environ 3:131

Batten SD, Ostle C, Hélaouët P, Walne AW (2022) Responses of Gulf of Alaska plankton communities to a marine heat wave. Deep Sea Res II 195:105002

Beardall J, Stojkovic S, Larsen S (2009) Living in a high CO_2 world: impacts of global climate change on marine phytoplankton. Plant Ecol Divers 2:191–205

Beaugrand G, Conversi A, Atkinson A, Cloern J and others (2019) Prediction of unprecedented biological shifts in the global ocean. Nat Clim Chang 9:237–243

Benedetti-Cecchi L (2021) Complex networks of marine heatwaves reveal abrupt transitions in the global ocean. Sci Rep 1 1:1739

Bertram DF, Harfenist A, Smith BD (2005) Ocean climate and El Niño impacts on survival of Cassin's auklets from upwelling and downwelling domains of British Columbia. Can J Fish Aquat Sci 62:2841–2853

Blight LK, Hobson KA, Kyser TK, Arcese P (2015) Changing gull diet in a changing world: a 150-year stable isotope ($\delta^{13}C$, $\delta^{15}N$) record from feathers collected in the Pacific Northwest of North America. Glob Change Biol 21: 1497–1507

Bodenstein B, Beckmen K, Sheffield G, Kuletz K, Van Hemert C, Berlowski B, Shearn-Bochsler V (2015) Avian cholera causes marine bird mortality in the Bering Sea of Alaska. J Wildl Dis 51:934–937

Boersma PD, Rebstock GA (2014) Climate change increases reproductive failure in Magellanic penguins. PLOS ONE 9:e85602

Braganza K, Gergis JL, Power SB, Risbey JS, Fowler AM (2009) A multiproxy index of the El Niño–Southern Oscillation, AD 1525–1982. J Geophys Res Atmos 114: D05106

Brown CJ, Fulton EA, Hobday AJ, Matear RJ (2010) Effects of climate-driven primary production change on marine food webs: implications for fisheries and conservation. Glob Change Biol 16:1194–1212

Bryndum-Buchholz A, Tittensor DP, Blanchard JL, Cheung WW and others (2019) Twenty-first-century climate change impacts on marine animal biomass and ecosystem structure across ocean basins. Glob Change Biol 25: 459–472

Burger AE, Piatt JF (1990) Flexible time budgets in breeding common murres: buffers against variable prey availability. Stud Avian Biol 14:71–83

Burke CM, Montevecchi WA (2018) Taking the bite out of winter: common murres (*Uria aalge*) push their dive limits to surmount energy constraints. Front Mar Sci 5:63

Cairns DK (1988) Seabirds as indicators of marine food supplies. Biol Oceanogr 5:261–271

Capotondi A, Newman M, Xu T, Di Lorenzo E (2022) An optimal precursor of northeast Pacific marine heatwaves and central Pacific El Niño events. Geophys Res Lett 49: e2021GL097350

Carvalho KS, Smith TE, Wang S (2021) Bering Sea marine heatwaves: patterns, trends and connections with the Arctic. J Hydrol (Amst) 600:126462

Chen Z, Shi J, Liu Q, Chen H, Li C (2021) A persistent and intense marine heatwave in the Northeast Pacific during 2019–2020. Geophys Res Lett 48:p.e2021GL093239

Cook TR, Martin R, Roberts J, Häkkinen H and others (2020) Parenting in a warming world: thermoregulatory responses to heat stress in an endangered seabird. Conserv Physiol 8:coz109

Di Lorenzo E, Mantua N (2016) Multi-year persistence of the 2014/15 North Pacific marine heatwave. Nat Clim Chang 6:1042–1047

Frederiksen M, Edwards M, Richardson AJ, Halliday NC, Wanless S (2006) From plankton to top predators: bottom-up control of a marine food web across four trophic levels. J Anim Ecol 75:1259–1268

Frederiksen M, Daunt F, Harris MP, Wanless S (2008) The demographic impact of extreme events: stochastic weather drives survival and population dynamics in a long-lived seabird. J Anim Ecol 77:1020–1029

Frölicher TL, Fischer EM, Gruber N (2018) Marine heatwaves under global warming. Nature 560:360–364

Furness RW, Camphuysen K (1997) Seabirds as monitors of the marine environment. ICES J Mar Sci 54:726–737

Gao G, Zhao X, Jiang M, Gao L (2021) Impacts of marine heatwaves on algal structure and carbon sequestration in conjunction with ocean warming and acidification. Front Mar Sci 8:758651

Gissi E, Manea E, Mazaris AD, Fraschetti S and others (2021) A review of the combined effects of climate change and other local human stressors on the marine environment. Sci Total Environ 755:142564

Gladics AJ, Suryan RM, Parrish JK, Horton CA, Daly EA, Peterson WT (2015) Environmental drivers and reproductive consequences of variation in the diet of a marine predator. J Mar Syst 146:72–81

Glencross JS, Lavers JL, Woehler EJ (2021) Breeding success of short-tailed shearwaters following extreme environmental conditions. Mar Ecol Prog Ser 672:193–203

Grebmeier JM, Maslowski W (2014) The Pacific Arctic region: an introduction. In: Grebmeier JM, Maslowski W (ed) The Pacific Arctic region. Springer, Dordrecht, p 1–15

Gurgel CFD, Camacho O, Minne AJP, Wernberg T, Coleman MA (2020) Marine heatwave drives cryptic loss of genetic diversity in underwater forests. Curr Biol 30:1199–1206

Hass T, Parrish JK (2002) Beached birds: COASST field guide. Wavefall Press, Seattle, WA

Hatch SA, Meyers PM, Mulcahy DM, Douglas DC (2000) Performance of implantable satellite transmitters in diving seabirds. Waterbirds 23:84–94

Hatch SA, Gill VA, Mulcahy DM (2010) Individual and colony-specific wintering areas of Pacific northern fulmars (*Fulmarus glacialis*). Can J Fish Aquat Sci 67:386–400

Häussermann V, Gutstein CS, Bedington M, Cassis D and others (2017) Largest baleen whale mass mortality during strong El Niño event is likely related to harmful toxic algal bloom. PeerJ 5:e3123

Hedd A, Montevecchi WA, Otley H, Phillips RA, Fifield DA (2012) Trans-equatorial migration and habitat use by sooty shearwaters *Puffinus griseus* from the South Atlantic during the nonbreeding season. Mar Ecol Prog Ser 449:277–290

Heinze C, Blenckner T, Martins H, Rusiecka D and others (2021) The quiet crossing of ocean tipping points. Proc Natl Acad Sci USA 118:e2008478118

Hipfner JM, Galbraith M, Bertram DF, Green DJ (2020) Basin-scale oceanographic processes, zooplankton community structure, and diet and reproduction of a sentinel North Pacific seabird over a 22-year period. Prog Oceanogr 182:102290

Hobday AJ, Alexander LV, Perkins SE, Smale DA and others (2016) A hierarchical approach to defining marine heatwaves. Prog Oceanogr 141:227–238

Hodder J, Graybill MR (1985) Reproduction and survival of seabirds in Oregon during the 1982–1983 El Niño. Condor 87:535–541

Holbrook NJ, Sen Gupta A, Oliver ECJ, Hobday AJ and others (2020) Keeping pace with marine heatwaves. Nat Rev Earth Environ 1:482–493

Holsman KK, Aydin K (2015) Comparative methods for evaluating climate change impacts on the foraging ecology of Alaskan groundfish. Mar Ecol Prog Ser 521: 217–235

Humphries GRW, Velarde E, Anderson DW, Haase B, Sydeman WJ (2015) Seabirds as early warning indicators of climate events in the Pacific. PICES Press 23:18–20

Hunt GL Jr (1990) The pelagic distribution of marine birds in a heterogeneous environment. Polar Res 8:43–54

Huntington HP, Danielson SL, Wiese FK, Baker M and others (2020) Evidence suggests potential transformation of the Pacific Arctic ecosystem is underway. Nat Clim Chang 10:342–348

Jeffries MO, Overland JE, Perovich DK (2013) The Arctic shifts to a new normal. Phys Today 66:35

Jessup DA, Miller MA, Ryan JP, Nevins HM and others (2009) Mass stranding of marine birds caused by a surfactant-producing red tide. PLOS ONE 4:e4550

Johns ME, Warzybok P, Jahncke J, Doak P, Lindberg M, Breed GA (2022) Episodes of high recruitment buffer against climate-driven mass mortality events in a North Pacific seabird population. J Anim Ecol 91:345–355

Jones T, Parrish JK, Punt AE, Trainer VL and others (2017) Mass mortality of marine birds in the Northeast Pacific caused by *Akashiwo sanguinea.* Mar Ecol Prog Ser 579: 111–127

Jones T, Parrish JK, Peterson WT, Bjorkstedt EP and others (2018) Massive mortality of a planktivorous seabird in response to a marine heatwave. Geophys Res Lett 45: 3193–3202

Jones T, Divine LM, Renner H, Knowles S and others (2019) Unusual mortality of tufted puffins (*Fratercula cirrhata*) in the eastern Bering Sea. PLOS ONE 14:e0216532

Killeen H, Dorman J, Sydeman W, Dibble C, Morgan S (2022) Effects of a marine heatwave on adult body length of three numerically dominant krill species in the California Current Ecosystem. ICES J Mar Sci 79: 761–774

Knowles S, Bodenstein BL, Berlowski-Zier BM, Thomas SM, Pearson SF, Lorch JM (2019) Detection of bisgaard taxon 40 in rhinoceros auklets (*Cerorhinca monocerata*) with pneumonia and septicemia from a mortality event in Washington, USA. J Wildl Dis 55:246–249

Kotzerka J, Hatch SA, Garthe S (2011) Evidence for foraging-site fidelity and individual foraging behavior of pelagic cormorants rearing chicks in the Gulf of Alaska. Condor 113:80–88

Laufkötter C, Zscheischler J, Frölicher TL (2020) High-impact marine heatwaves attributable to human-induced global warming. Science 369:1621–1625

Ledet J, Campbell H, Byrne M, Poore AG (2021) Differential tolerance of species alters the seasonal response of marine epifauna to extreme warming. Sci Total Environ 797: 149215

Lee DE, Nur N, Sydeman WJ (2007) Climate and demography of the planktivorous Cassin's auklet *Ptychoramphus aleuticus* off northern California: implications for population change. J Anim Ecol 76:337–347

Lim YK, Kovach RM, Pawson S, Vernieres G (2017) The 2015/16 El Niño event in context of the MERRA-2 reanalysis: a comparison of the tropical Pacific with 1982/83 and 1997/98. J Clim 30:4819–4842

Montevecchi WA, Regular PM, Rail JF, Power K and others (2021) Ocean heat wave induces breeding failure at the southern breeding limit of the northern gannet *Morus bassanus.* Mar Ornithol 49:71–78

Mueter FJ, Weems J, Farley EV, Sigler MF (2017) Arctic ecosystem integrated survey (Arctic Eis): marine ecosystem dynamics in a rapidly changing Pacific Arctic Gateway. Deep Sea Res II 135:1–6

Nur N, Jahncke J, Herzog MP, Howar J and others (2011) Where the wild things are: predicting hotspots of seabird aggregations in the California Current System. Ecol Appl 21:2241–2257

O'Hara PD, Morgan KH (2006) Do low rates of oiled carcass recovery in beached bird surveys indicate low rates of ship-source oil spills? Mar Ornithol 34:133–140

Osborne OE, Hara PD, Whelan S, Zandbergen P, Hatch SA, Elliott KH (2020) Breeding seabirds increase foraging range in response to an extreme marine heatwave. Mar Ecol Prog Ser 646:161–173

Österblom H, Casini M, Olsson O, Bignert A (2006) Fish, seabirds and trophic cascades in the Baltic Sea. Mar Ecol Prog Ser 323:233–238

Parrish JK, Marvier M, Paine RT (2001) Direct and indirect effects: interactions between bald eagles and common murres. Ecol Appl 11:1858–1869

Parrish JK, Bond N, Nevins H, Mantua N, Loeffel R, Peterson WT, Harvey JT (2007) Beached birds and physical forcing in the California Current system. Mar Ecol Prog Ser 352:275–288

Piatt JF, Van Pelt TI (1997) Mass-mortality of guillemots (*Uria aalge*) in the Gulf of Alaska in 1993. Mar Pollut Bull 34: 656–662

Piatt JF, Drew G, Van Pelt T, Abookire A, Nielsen JL, Shultz M, Kitaysky A (1999) Biological effects of the 1997/98 ENSO in Cook Inlet, Alaska. PICES Sci Rep 10:93–99

Piatt JF, Sydeman WJ, Wiese F (2007a) Introduction: a modern role for seabirds as indicators. Mar Ecol Prog Ser 352: 199–204

Piatt JF, Harding AMA, Shultz M, Speckman SG, Van Pelt TI, Drew GS, Kettle AB (2007b) Seabirds as indicators of marine food supplies: Cairns revisited. Mar Ecol Prog Ser 352:221–234

Piatt JF, Parrish JK, Renner HM, Schoen SK and others (2020) Extreme mortality and reproductive failure of common murres resulting from the Northeast Pacific marine heatwave of 2014–2016. PLOS ONE 15:e0226087

Pinheiro J, Bates D, R Core Team (2022) nlme: linear and nonlinear mixed effects models. R package version 3.1-157. https://CRAN.R-project.org/package=nlme

Pya N (2022) scam: shape constrained additive models. R package version 1.2-13. https://CRAN.R-project.org/package=scam

R Core Team (2022) R: a language and environment for statistical computing. R Foundation for Statistical Computing, Vienna

Reynolds RW, Rayner NA, Smith TM, Stokes DC, Wang W (2002) An improved *in situ* and satellite SST analysis for climate. J Clim 15:1609–1625

Romano MD, Renner HM, Kuletz KJ, Parrish JK and others (2020) Die-offs, reproductive failure, and changing at-sea abundance of murres in the Bering and Chukchi Seas in 2018. Deep Sea Res II 181–182:104877

Ryan JP, Kudela RM, Birch JM, Blum M and others (2017) Causality of an extreme harmful algal bloom in Monterey Bay, California, during the 2014–2016 northeast Pacific warm anomaly. Geophys Res Lett 44:5571–5579

Samhouri JF, Feist BE, Fisher MC, Liu O and others (2021) Marine heatwave challenges solutions to human–wildlife conflict. Proc R Soc B 288:20211607

Sanford E, Sones JL, García-Reyes M, Goddard JHR, Largier JL (2019) Widespread shifts in the coastal biota of northern California during the 2014–2016 marine heatwaves. Sci Rep 9:4216

Santora JA, Mantua NJ, Schroeder ID, Field JC and others (2020) Habitat compression and ecosystem shifts as potential links between marine heatwave and record whale entanglements. Nat Commun 11:536

Scannell HA, Pershing AJ, Alexander MA, Thomas AC, Mills KE (2016) Frequency of marine heatwaves in the North Atlantic and North Pacific since 1950. Geophys Res Lett 43:2069–2076

Schoen SK, Arimitsu ML, Marsteller CE, Piatt JF (2022) Lingering impacts of the 2014–2016 northeast Pacific marine heatwave on seabird demography in Cook Inlet, Alaska (USA). Mar Ecol Prog Ser, doi:10.3354/meps14177

Simpson G (2022) gratia: graceful ggplot-based graphics and other functions for GAMs fitted using mgcv. R package version 0.7.3. https://gavinsimpson.github.io/gratia/

Sinclair EH, Vlietstra LS, Johnson DS, Zeppelin TK and others (2008) Patterns in prey use among fur seals and

seabirds in the Pribilof Islands. Deep Sea Res II 55: 1897–1918

Smale DA, Wernberg T, Oliver ECJ, Thomsen M and others (2019) Marine heatwaves threaten global biodiversity and the provision of ecosystem services. Nat Clim Chang 9:306–312

Smith KE, Burrows MT, Hobday AJ, King NG and others (2023) Biological impacts of marine heatwaves. Annu Rev Mar Sci 15:119–145

Stabeno PJ, Bell SW (2019) Extreme conditions in the Bering Sea (2017–2018): record-breaking low sea-ice extent. Geophys Res Lett 46:8952–8959

Stabeno PJ, Duffy-Anderson JT, Eisner LB, Farley EV, Heintz RA, Mordy CW (2017) Return of warm conditions in the southeastern Bering Sea: physics to fluorescence. PLOS ONE 12:e0185464

Stan Development Team (2022a) Stan modeling language user's guide and reference manual, version 2.30. https://mc-stan.org

Stan Development Team (2022b) RStan: the R interface to Stan. R package version 2.26.13. https://mc-stan.org/users/interfaces/rstan.html

Stocker TF, Qin D, Plattner GK, Tignor M and others (eds) (2013) IPCC, 2013: climate change 2013: the physical science basis. Contribution of Working Group I to the Fifth Assessment Report of the Intergovernmental Panel on Climate Change. Cambridge University Press, Cambridge

Suryan RM, Irons DB, Brown ED, Jodice PG, Roby DD (2006) Site-specific effects on productivity of an upper trophic-level marine predator: bottom-up, top-down, and mismatch effects on reproduction in a colonial seabird. Prog Oceanogr 68:303–328

Suryan RM, Arimitsu ML, Coletti HA, Hopcroft RR and others (2021) Ecosystem response persists after a prolonged marine heatwave. Sci Rep 11:6235

Sydeman WJ, Schoeman DS, Thompson SA, Hoover BA and others (2021) Hemispheric asymmetry in ocean change and the productivity of ecosystem sentinels. Science 372: 980–983

Tate HM, Studholme KR, Domalik AD, Drever MC and others (2021) Interannual measures of nutritional stress during a marine heatwave (the Blob) differ between two North Pacific seabird species. Conserv Physiol 9:coab090

Tuck GN, Thomson RB, Barbraud C, Delord K, Louzao M, Herrera M, Weimerskirch H (2015) An integrated assessment model of seabird population dynamics: Can individual heterogeneity in susceptibility to fishing explain abundance trends in Crozet wandering albatross? J Appl Ecol 52:950–959

Van Hemert C, Schoen SK, Litaker RW, Smith MM and others (2020) Algal toxins in Alaskan seabirds: evaluating the role of saxitoxin and domoic acid in a large-scale die-off of common murres. Harmful Algae 92:101730

Vehtari A, Gelman A, Simpson D, Carpenter B, Bürkner PC (2021) Rank-normalization, folding, and localization: an improved R for assessing convergence of MCMC (with discussion). Bayesian Anal 16:667–718

Watanuki Y, Ishikawa K, Takahashi A, Kato A (2004) Foraging behavior of a generalist marine top predator, Japanese cormorants (*Phalacrocorax filamentosus*), in years of demersal versus epipelagic prey. Mar Biol 145:427–434

Watanuki Y, Yamamoto M, Okado J, Ito M, Sydeman W (2022) Seabird reproductive responses to changing climate and prey communities are mediated by prey packaging. Mar Ecol Prog Ser 683:179–194

Wiese FK (2003) Sinking rates of dead birds: improving estimates of seabird mortality due to oiling. Mar Ornithol 31: 65–70

Will A, Thiebot JB, Ip H, Shoogukwruk P and others (2020a) Investigation of the 2018 thick-billed murre (*Uria lomvia*) die-off on St. Lawrence Island rules out food shortage as the cause. Deep Sea Res II 181–182:104879

Will A, Takahashi A, Thiebot JB, Martinez A and others (2020b) The breeding seabird community reveals that recent sea ice loss in the Pacific Arctic does not benefit piscivores and is detrimental to planktivores. Deep Sea Res II 181–182:104902

Wood SN (2017) Generalized additive models: an introduction with R (2nd edn). CRC Press, Boca Raton, FL

Wood KR, Wang J, Salo SA, Stabeno PJ (2015) The climate of the Pacific Arctic during the first RUSALCA decade 2004–2013. Oceanography (Wash DC) 28:24–35

Woodworth-Jefcoats PA, Polovina JJ, Drazen JC (2017) Climate change is projected to reduce carrying capacity and redistribute species richness in North Pacific pelagic marine ecosystems. Glob Change Biol 23:1000–1008

Editorial responsibility: John F. Piatt (Guest Editor), Anchorage, Alaska, USA
Reviewed by: W. Montevecchi and 2 anonymous referees

Submitted: November 16, 2022
Accepted: May 15, 2023
Proofs received from author(s): June 30, 2023